Clean Technologies and Environmental Policy (2026) 28:216
https://doi.org/10.1007/s10098-026-03468-x

ORIGINAL PAPER

From solar radiation to green methanol: an energy efficiency of electricity- and biomass-based provision pathways

Marvin Scherzinger[1] · Wolfram Tuschewitzki[1] · Stefan Bube[1] · Martin Kaltschmitt[1]

Received: 20 August 2025 / Accepted: 16 March 2026

Abstract

With sunlight as an energy source, carbon-based products can be produced from atmospheric carbon without relying on fossil resources. Thus, one electricity- and two bio-based carbon dioxide utilization options are compared exemplarily for the provision of methanol. The energy requirements of each pathway and the included sub-steps are assessed based on theoretical and state-of-the-art efficiencies to allow for a fair comparison of the overall energy balance and to assess the energetic value of biomass. The results show that the investigated power-based pathway has a higher energy efficiency under ideal conditions (i.e., 23.5%) compared to the options involving biomass production (3.8 to 4.4%). This also holds true for present-day process efficiencies (i.e., 9.4% for power-based pathway and 0.27 to 0.56% for biomass-based pathways). The higher energy demand within the biomass-based pathway is mainly caused by the low photosynthetic efficiency responsible for biomass production. If biomass production energy is excluded, such as when using waste biomass, the biomass-based pathway becomes energetically advantageous (i.e., efficiencies between 74.3 and 83.9% under ideal conditions and of 27.4 and 47.4% under currently feasible frame conditions). Based on the presented calculations, a specific energetic value is assigned to biomass, indicating the potential energy savings achieved by biomass utilization (i.e., 2.9 to 3.1 $\mathrm{kJ\,kJ^{-1}_{CH_3OH}}$. under ideal conditions and 7.1 to 11.5 $\mathrm{kJ\,kJ^{-1}_{CH_3OH}}$. under present-day conditions). This work lays the foundation for further analyses of these pathways and their multifaceted benefits and drawbacks beyond purely energetic considerations.

✉ Marvin Scherzinger
marvin.scherzinger@tuhh.de

Wolfram Tuschewitzki
wolfram.tuschewitzki@tuhh.de

Stefan Bube
stefan.bube@tuhh.de

Martin Kaltschmitt
kaltschmitt@tuhh.de

[1] Institute of Environmental Technology and Energy Economics, Hamburg University of Technology (TUHH), Eissendorfer Str. 40, 21073 Hamburg, Germany

Published online: 07 August 2026

Graphical Abstract

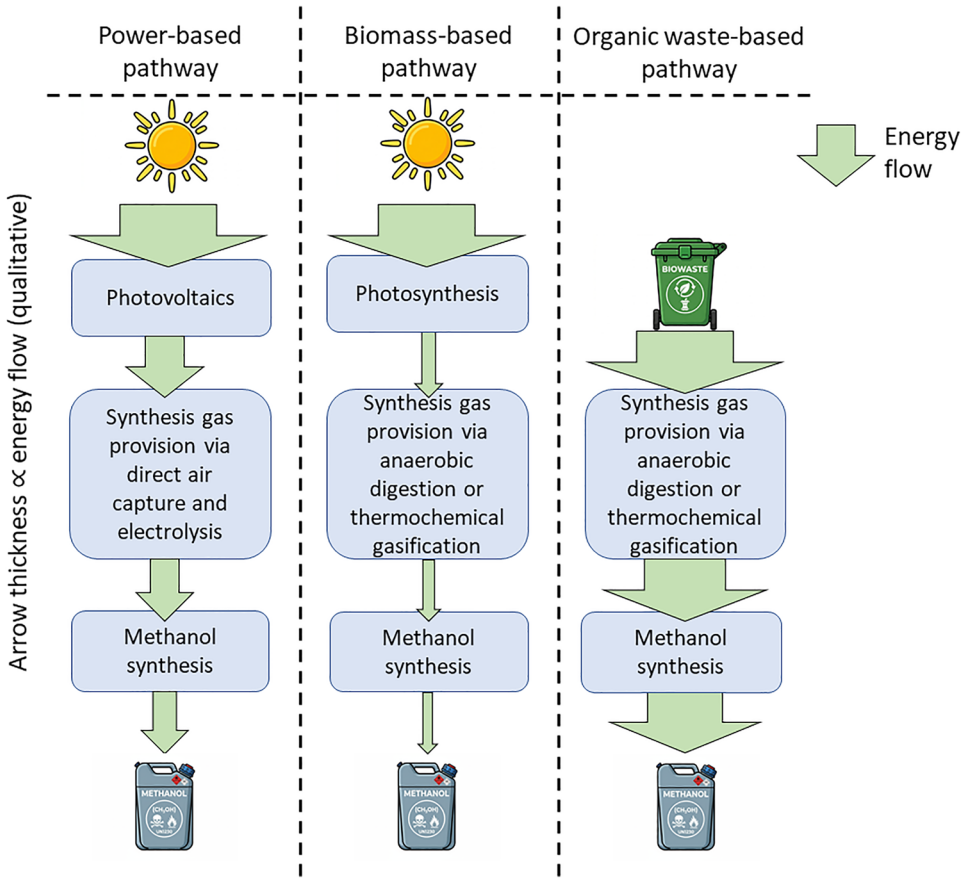

Keywords Photovoltaics · Photosynthesis · Direct air capture · Anaerobic digestion · Thermochemical gasification · Electrolysis · Methanol synthesis

Abbreviations

AM	Air mass
C	Carbon
CAM	Crassulacean acid metabolism
CH_4	Methane
CH_3OH	Methanol
$C_6H_{12}O_6$	Glucose
CO_2	Carbon dioxide
DAC	Direct air capture
GHG	Greenhouse gases
H	Hydrogen
H_2O	Water
HHV	Higher heating value
NRTL	Non-random two liquid
O	Oxygen
PAR	Photosynthetically active region
PGA	3-Phosphoglycerate
PV	Photovoltaic
RuBisCO	Ribulose-1,5-bisphosphate carboxylase/oxygenase
WGS	Water gas shift

Introduction

Carbon-containing greenhouse gases (GHGs) such as carbon dioxide (CO_2) from fossil sources contribute significantly to anthropogenic climate change (Kweku et al. 2018). Therefore, decarbonization measures need to be implemented to limit global warming to an endurable level. As a consequence, efforts are currently being made to transform the energy sector in particular. Here, market-ready alternatives are already available (e.g., wind turbines, photovoltaic systems) to decarbonize resp. defossilize this sector and thus to release less CO_2 originating from fossil fuels into the atmosphere. However, besides

the energy sector, high CO_2 emissions also occur in other sectors.

- Mobility: At present, mainly carbon-based fuels are used to generate kinetic energy for transportation purposes via fuel combustion and subsequent mechanical conversion of the released energy. In the land transport, a transformation toward direct electrification (decarbonization) of vehicles has begun—this has not yet taken place in the aviation and maritime mobility as well as land-based heavy-duty transportation and with special purpose vehicles (e.g., tractors, excavators) due to operational and technical limitations.
- Chemical industry: CO_2 is released during the provision of process energy in the chemical industry (e.g., combustion of carbon-based fuels to provide thermal energy). Furthermore, carbon is the basis of organic chemistry and is a major component in many chemicals and polymers. Most of this carbon also originates from the utilization of fossil fuel resources and is therefore usually released as additional CO_2 at the end of the product life cycle.
- Construction industry: Carbon-containing minerals are mined (e.g., limestone). During the process of deacidification being essential in cement production, significant amounts of fossil CO_2 are released from these minerals and emitted into the atmosphere. In addition, a large proportion of the required energy for the provision of process heat needed is generated from fossil fuels, leading to further CO_2 emissions.

The aforementioned explains why there is often a strong focus on the energy sector when it comes to decarbonization. But, compared to other sectors of our highly interconnected economy, the energy sector can be decarbonized relatively easily in theory. However, in many other sectors, it is very challenging to avoid the use of carbon as there are so far no substitutes for it. Furthermore, a closed carbon cycle, in which released CO_2 is captured and recycled, is not always possible, especially with diffuse sources and/or numerous small-scale applications. However, due to the relatively small carbon flow in the long-term natural carbon cycle, humanity cannot rely on nature to reduce the carbon stock in the atmosphere to stop short time climate change. (For more information, see supplementary material.)

This challenging situation results in the necessity for a transition from the use of fossil carbon-containing raw materials such as coal, crude oil, and natural gas to the use of renewable carbon compounds (i.e., defossilization) to counterbalance unavoidable GHG emissions within such sectors (IPCC 2023). To produce renewable sourced carbon compounds, both raw materials and energy are required.

Against this background, in recent years, several studies have focused on the production of fossil-free fuels, such as green methanol. For instance, one study explored the design of methanol production systems by integrating direct air capture (DAC) technology with electricity from wind power plants (Fulham et al. 2024). Another investigation examined advanced power-to-methanol processes, demonstrating that heat-assisted systems can improve efficiency and make renewable methanol economically viable compared to fossil fuels (Zhang et al. 2025). Moreover, another study introduced an innovative flow reactor that combines CO_2 capture with light-driven conversion to syngas, enabling on-site production of renewable fuels from air-captured CO_2 (Kar et al. 2025). This indicates a considerable interest in solutions of this kind. Aligned with these efforts, a recent study confirms that Europe can feasibly scale up green methanol production from solar-derived hydrogen by integrating existing natural gas infrastructure and hydrogen blending, thereby achieving noteworthy CO_2 reductions when supported by strategic investments and policies (Rodriguez-Pastor et al. 2025). A study by Zhao et al. (Zhao et al. 2025) exploring different methanol-to-electricity pathways and their market potential exemplifies a broader trend in the literature: While economic challenges and technical hurdles (such as the need for cost reductions and technological breakthroughs) are well recognized, fundamental comparisons considering physicochemical efficiency limits tend to be highly case-specific and dependent on factors such as the chosen scale of implementation. What remains absent in the existing literature is an estimation of such pathways based solely on their underlying physical principles, a necessary step to reveal the highest possible theoretical efficiency.

Our research focuses on this challenge by aiming to quantify the theoretical energy efficiency of a fossil-free fuel production system powered by renewable energy, utilizing existing technologies that capture carbon from the atmosphere through DAC or photosynthesis. This will then be compared with present-day efficiencies that can already be achieved today. Thereby, we strive to offer broadly applicable conclusions that extend beyond the specific cases addressed in the previously mentioned studies.

Below, the solar spectrum being the basis to cover the need for renewable energy, is presented. Based on this, the specific research objectives of this paper are derived and discussed.

Solar spectrum

The Sun emits electromagnetic radiation covering a broad wavelength range. The emitted energy (B) per wavelength

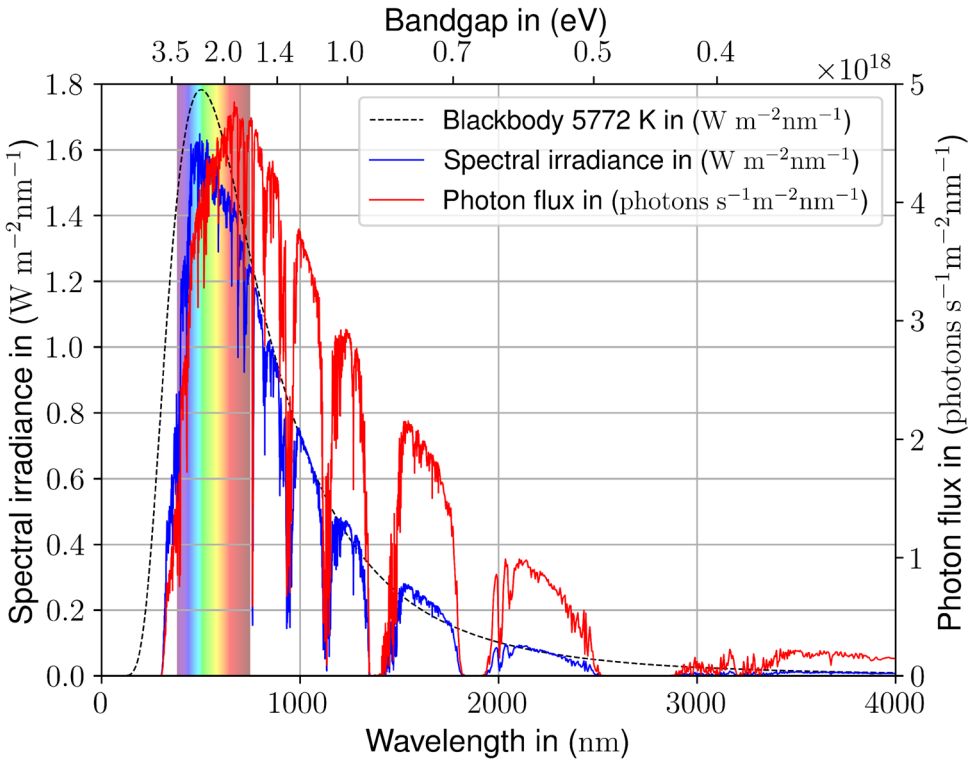

Fig. 1 Spectrum of terrestrial solar irradiance and photon flux. Approximated black body radiation spectrum (black, dashed)—$T_S = 5772$ K—and reference air mass (AM) 1.5 spectrum (ASTM G-173) spectral irradiance (blue) with corresponding photon flux (red). The section of the spectrum visible to humans (violet to red) is shown in the background for reference

(λ) depends on the temperature of the emitter as described by Planck's radiation law (Eq. 1). Thus, the electromagnetic radiation power is defined as a function of wavelength with Planck's constant ($h = 6.626 \cdot 10^{-34}$ J s), the speed of light in vacuum ($c = 2.998 \cdot 10^{8}$ m s^{-1}), and the Boltzmann constant ($k_B = 1.381 \cdot 10^{-23}$ J K^{-1}). The spectrum of the Sun can be approximated via Eq. 1 with an effective black body temperature of $T_S = 5\,772$ K (Prša et al. 2016).

$$B_\lambda(\lambda, T) = \frac{2\,h\,c^2}{\lambda^5} \frac{1}{\exp\left(\frac{h\,c}{\lambda\,T_S\,k_B}\right) - 1} \tag{1}$$

Radiative energy (E_g) is emitted in quanta—photons—whose energy is proportional to their frequency (ν) and inversely proportional to their wavelength (λ) (Eq. 2).

$$E_g = h\,\nu = \frac{h\,c}{\lambda} \tag{2}$$

As the Sun emits its radiation in all directions, only a certain quantity of the emitted photons (the spectrum) reaches the outer rim of Earth's atmosphere. This spectrum can be calculated using an intensity factor via Eq. 3 by squaring the quotient of the solar radius ($R_\odot = 6.957 \cdot 10^{8}$ m (Prša et al. 2016)) and the mean distance between the Sun and the Earth (i.e., one astronomical unit (AU); $1AU \approx 1.496 \cdot 10^{11}$ m (Prša et al. 2016)). Since the light reaches only one hemisphere of the Earth, multiplication by the geometrical factor π is required. The resulting extraterrestrial spectral irradiance for a black body temperature of the Sun of $T_S = 5\,772$ K is shown as a black, dashed line in Fig. 1.

$$f_I = \left(\frac{R_\odot}{1\,AU}\right)^2 \approx 4.6 \cdot 10^{-4} \tag{3}$$

However, not all photons that reach the outer rim of the Earth's atmosphere reach the surface of the Earth (and thus the leaf of a plant or the surface of a solar cell). The spectrum is attenuated and changed in shape by absorption and scattering of the solar radiation within the atmosphere (i.e., on the way from the outer rim of the atmosphere to the Earth's surface).

- The main contributors to absorption effects are water vapor, carbon dioxide, methane, ozone, and nitrogen oxide (Nelson 2010).
- Scattering is realized due to the diversion of radiation at particles with a radius significantly smaller than the wavelength of the incident light (Rayleigh scattering) as well as the diversion of radiation at particles with a

radius in the wavelength of light and larger (Mie scattering) (Newton 1982).

Attenuation is approximated by utilizing the air mass factor (Eq. 4), a measure of how much atmosphere sunlight passes through on average before reaching the Earth's surface, expressed as a ratio relative to the shortest possible path length (at zenith) with θ being the angle between the vertical and the actual light (Würfel 2010).

$$AM = \frac{1}{\cos(\theta)} \tag{4}$$

The actual irradiance at the Earth's surface varies by location and time due to changes, e.g., in atmospheric conditions, time of day, season, and ecliptic (the apparent path of the Sun across the sky). Because many optical phenomena are dependent on the wavelength, reference spectra have been defined to standardize measurements and allow for fair comparisons (e.g., for benchmarking) (International Organization for Standardization 2022). A reference spectrum does not factor in daily or seasonal variability and does not represent the integration of solar radiation over a year; it basically describes the maximum energy available on the surface of the Earth.

Research objectives

If only carbon sources of the short carbon cycle (see supplementary material) are to be used, on the one hand, CO_2 can be extracted directly from the atmosphere using technical measures (i.e., direct air capture (DAC)); this CO_2 can then be converted into a well-usable form (e.g., methane (CH_4) or methanol (CH_3OH)) by means of heat-supported chemical syntheses. On the other hand, the carbon bound in organic substances (i.e., biomass) can be utilized; this carbon ultimately originates from CO_2 assimilated via natural photosynthesis also from the atmosphere. Within biomass, the carbon is not present in a fully oxidized form as CO_2, but chemically bound within a wide variety of compounds, containing mainly carbon (C), hydrogen (H), and oxygen (O).

Thus, in the case of biomass nature provides a certain amount of synthesis input. The respective biogenic carbon–hydrogen–oxygen molecules (e.g., cellulose, hemicellulose, and lignin) can then be converted into a targeted product by technical means. In contrast, when using atmospheric CO_2, the energy for the upconcentration of carbon, as well as for the provision of hydrogen, must be provided by additional energy (in most cases electrical energy). In both cases, for the subsequent downstream conversion up to a final usable carbon-containing product, further energy is needed, whereby these additional downstream steps might differ greatly depending on whether biomass or atmospheric CO_2 is used.

Keeping this in mind, the aim of this paper is a comparison of different options to produce a carbonaceous product (here: methanol) from atmospheric CO_2 in terms of energy demand along the entire conversion pathway. In the first case, CO_2 fixation is realized via photosynthesis (i.e., biomass buildup), and in the second case, CO_2 is extracted via direct air capture (DAC) units from ambient air. In order to ensure comparability, the assessment limits are chosen in such a way that the energy supply always originates from the solar spectrum (Fig. 1). The system boundaries/assessment limits are set in a way that all conversion steps from the solar radiation reaching the Earth's surface to the end product (here: methanol) are considered (Fig. 2). The additional water required for methanol production is assumed to be available without considering additional energetic efforts.

By gradually determining the energy efficiencies/energy losses of the individual conversion steps involved (Fig. 2), an overall energy efficiency can ultimately be calculated for each pathway. This is done firstly on the basis of the physically/chemically achievable maxima (i.e., theoretically achievable maximum energy efficiency; hereinafter referred to as theoretical efficiency). These theoretical efficiencies are based on the theoretical optima/on idealized assumptions (Sect. "Energy efficiency assessment") only achievable under ideal conditions. Thus, for comparison, present-day achievable energy efficiencies based on literature values (hereinafter referred to as present-day efficiency) are also given for each process step.

Various conversion processes take place in each of the processes under consideration. When determining the theoretical efficiencies, only the energy losses in the individual processes are estimated; any energy required to set up the systems, as well as possible energy recovery strategies (e.g., heat integration), is not taken into account. All efficiencies are based on the higher heating value. The theoretical efficiencies, therefore, ultimately reflect the maximum physically/chemically achievable efficiency for each process step.

In order to analyze how far reality is away from the theoretical maximum under current conditions, a comparison is made with present-day technologies. Thereby, conservative values possible to be achieved today are considered; location specific effects and seasonal fluctuations, among others, are not taken into account.

Based on the obtained results, statements are made about the framework conditions under which the respective pathways are promising or less promising for producing methanol from an energy balance point of view.

In summary, this means that the study explicitly emphasizes three central aspects. First, it applies a consistent

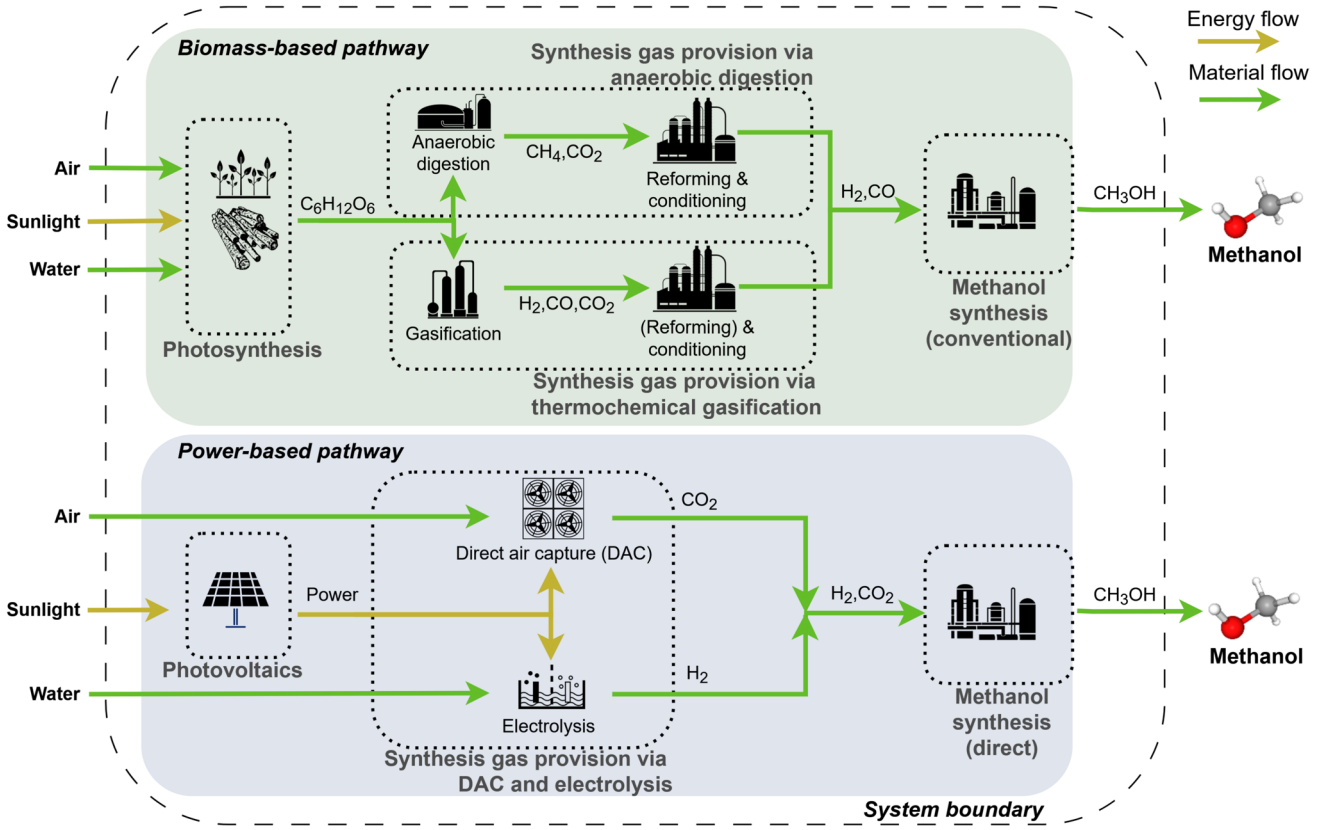

Fig. 2 Methanol production pathways

solar-to-methanol system boundary to both biomass-based and power-based pathways, ensuring a fair and transparent comparison. Second, it contrasts theoretical and current process efficiencies both step by step and at the overall system level. Third, it introduces the concept of the specific energetic value of biomass, providing an additional perspective for understanding the fundamental energetic differences between the two routes.

System description and limitations

The following consideration includes a purely power-based pathway (in which solar energy is first converted into electrical energy using photovoltaic systems) and a purely biomass-based pathway (in which solar energy is first used to build up biomass and all the process energy subsequently required is provided by this biogenic matter). For both pathways, no additional external energy is supplied beside solar energy. In order to ensure comparability between the processes themselves and with other studies, a reference spectrum (Sect. "Solar spectrum" and introduction of Sect. "Energy efficiency assessment") is selected providing the average yearly irradiance in temperate latitudes; i.e., seasonal and diurnal fluctuations cannot be taken into account based on this approach. Furthermore, within the biomass-based pathway, only the conversion of the carbohydrate glucose is considered on the downstream pathway toward methanol production (i.e., no further anabolic reactions are taken into account).

The basic principles of the individual system components (Fig. 2) are presented sequentially below. Based on these process steps, an energy assessment is then carried out subsequently in Sect. "Energy efficiency assessment."

Biomass-based pathway

Photosynthesis

Photosynthesis is a biochemical process in which photoautotrophic organisms synthesize organic compounds with the help of solar radiation and inorganic precursors. The overall photosynthesis can be subdivided into two sub-reactions (i.e., light reaction and dark reaction). Within the light reaction, the emitted sunlight is converted into chemical energy to be used in the subsequent dark reaction to convert

atmospheric CO_2 into organic molecules (Nugent 1996). (For more information, see supplementary material.)

The reaction of photosynthesis can be summarized in a gross equation, where CO_2 from the ambient air and water from the environment is converted into carbohydrates, with the primary product being glucose ($C_6H_{12}O_6$). As by-products, oxygen, and water are released into the environment (Eq. 5),

$$6\ CO_2 + 12\ H_2O \rightarrow C_6H_{12}O_6 + 6\ O_2 + 6\ H_2O \tag{5}$$

Synthesis gas production via anaerobic digestion

The next step in the process chain is the production of a carbonaceous gas. Biomass with a high water content is preferably converted into biogas, a gas mixture consisting mainly of methane and carbon dioxide, using the anaerobic digestion pathway. The assumption of this conversion pathway is justified by the process energy requirement (drying would entail a high energy requirement, making the thermochemical pathway unattractive for wet biomass) and by the conditions required during anaerobic conversion. (Due to biological reasons, a high water content is essential.) Below the basics of biogas production and the subsequent gas treatment (i.e., reforming and conditioning) are explained.

Anaerobic digestion. Under anaerobic conditions, organic matter can be degraded step by step by different microorganism groups (i.e., bacteria and archaea). The produced gas mixture varies depending on the biomass composition (Eq. 6); but methane and carbon dioxide make up the majority of the gas. Most digestion processes are realized within a medium-temperature range (approx. 37 °C) because they typically represent a good compromise between the time- and volume-dependent gas yield and the necessary process energy (heat) (Uddin and Wright 2023).

$$\begin{aligned} &C_nH_aO_b + \left(n - \frac{a}{4} - \frac{b}{2}\right)H_2O \\ &\rightarrow \left(\frac{n}{2} - \frac{a}{8} + \frac{b}{4}\right)CO_2 + \left(\frac{n}{2} + \frac{a}{8} - \frac{b}{4}\right)CH_4 \end{aligned} \tag{6}$$

Reforming and conditioning. Synthesis gas (syngas) is generated from biogas through reforming and conditioning processes.

- Reforming involves the conversion of light hydrocarbons into a raw synthesis gas composed mainly of CO and H_2 via partial oxidation, using various oxidizing agents (commonly O_2, H_2O, or CO_2).
- Conditioning adjusts the syngas composition to the required specification.

During reforming, a partial oxidation of methane takes place (Eq. 7, Eq. 8, Eq. 9). The composition of the respective product gases depends on the selected reforming process. The syngas composition can be adjusted to the demands of the subsequent synthesis (i.e., conditioning) through the choice and dosing of the employed oxidizing agents, as well as through the adjustment of the respective process conditions. Furthermore, conditioning is also possible using further reactions such as the water–gas shift (WGS) (Eq. 10), where the product gases from the reforming process are used as a reactant. In this case, a subsequent partial CO_2 removal is necessary.

$$CH_4 + \frac{1}{2}\ O_2 \rightleftharpoons CO + 2\ H_2 \tag{7}$$

$$CH_4 + H_2O \rightleftharpoons CO + 3\ H_2 \tag{8}$$

$$CH_4 + CO_2 \rightleftharpoons 2\ CO + 2\ H_2 \tag{9}$$

$$CO + H_2O \rightleftharpoons CO_2 + H_2 \tag{10}$$

Synthesis gas production via thermochemical gasification

If the biomass is available as a largely dry solid (lignocellulosic biomass like, e.g., wood and straw), a conversion into hydrogen and carbon monoxide via the thermochemical gasification pathway is more promising. Below, the basics of thermochemical gasification and the subsequent gas treatment are presented.

Thermochemical gasification. Via thermochemical gasification, solid biomass can be transferred into a high-calorific gas mixture known as product gas to be further conditioned to provide a syngas. The main gas components are carbon monoxide (CO), hydrogen (H_2), water vapor (H_2O), carbon dioxide (CO_2), and gaseous hydrocarbons (C_xH_y). The share of these various gas components varies greatly depending on, e.g., the gasification technology, the gasification agent as well as the composition of the biomass. Such a thermochemical gasification can be described by Eq. 11.

$$C_nH_aO_b + c(O_2) + d(H_2O) -> x(CO) + y(H_2) + z(CO_2) \tag{11}$$

Additionally, small quantities of solid carbon (coke, charcoal), ash, and condensable components (i.e., tars and oils) may be produced as by-products (Molino et al. 2016). Such a thermochemical gasification can be divided into three different steps.

1. Drying: The required thermal energy depends primarily on the water content of the biogenic feedstock. Drying takes place at temperatures of about 100 to 150 °C.

2. Pyrolytic decomposition: The biomass is heat-induced decomposed in the absence of oxygen at temperatures between 150 to 500 °C. Thereby, the carbonaceous biomass matrix is heat-induced destroyed by breaking chemical bonds. This results in the formation of fragments of the molecules originally contained within the biomass, including the desired gases. These small molecules are released into the surrounding gas phase (Molino et al. 2016).
3. Gasification: In the substoichiometric presence of oxygen, the remaining carbon (coke), which cannot be transferred into the gas phase within the pyrolytic decomposition due to thermodynamic/chemical constraints, is converted into gaseous compounds at temperatures of about 800 to 1 100 °C (Puig-Arnavat et al. 2010).

Gas conditioning. To adjust the synthesis gas composition, conditioning via a WGS reaction (Eq. 10) and a subsequent CO_2 removal is common. Depending on the biomass composition and the gasification process, CO_2 separation without an additional WGS reaction may also be sufficient.

Conventional methanol synthesis

The conventional methanol synthesis is a heterogeneously catalyzed conversion of the syngas components usually operated in a temperature and pressure range of 200 to 300 °C and 40 to 100 bar (Dieterich et al. 2020; Ott et al. 2012).

The respective formation of methanol can be described by Eq. 12.

$$CO + 2\ H_2 \rightleftharpoons CH_3OH \tag{12}$$

Due to the exothermic and volume-decreasing nature of the equilibrium-limited methanol formation reaction, product generation is favored by low temperatures and high pressures (Heer 1957). In addition, further side reactions might occur in parallel, including direct methanol synthesis (Eq. 14) and WGS (Eq. 10).

Power-based pathway

Solar cell

Solar or photovoltaic (PV) cells are able to convert light directly into electricity based on the photovoltaic effect. Such cells typically consist of a n- and a p-doped semiconductor material (e.g., silicon). The photons absorbed by this material generate electron–hole pairs through charge separation. These charge carriers are then separated by an internal electric field formed due to the differently doped material within the cell (i.e., negatively charged electrons accumulate on one side of the electrical field and positively charged holes on the other side). If these charge carriers are then discharged from the cell surface, a flow of electric current can be created (Würfel 2010). The electrical efficiency of a solar cell (i.e., the proportion of the irradiated sunlight it converts into usable electricity) is influenced, e.g., by material properties and manufacturing as well as the respective design and the installation.

Synthesis gas production via electrolysis and direct air capture

Synthesis gas for direct methanol synthesis (Sects. "Direct methanol synthesis" and "Direct methanol synthesis") (Sections 2.2.3 and 3.2.3) comprises hydrogen and carbon dioxide. Hydrogen can be provided via electrolysis devices, and carbon dioxide is supplied via direct air capture units. Both technologies are required in combination to produce the required gas mixture.

Electrolysis. Electrolysis realizes an electro-chemical molecule splitting process; i.e., water is split into hydrogen and oxygen Eq. 13 (Carmo et al. 2013). This process needs primarily electrical energy and, in some cases, additional heat.

$$H_2O \rightarrow H_2 + \frac{1}{2}\ O_2 \tag{13}$$

Direct air capture. Direct air capture (DAC) units aim to separate CO_2 from the atmosphere, where its concentration is currently ca. 420 ppm (Lan et al. 2024). Due to the low concentration of CO_2 in air, large volumes of air must pass through the DAC apparatus to capture meaningful amounts of CO_2 (Fasihi et al. 2019). The final products are CO_2 and a mixture of all other air components, mainly N and O_2. The necessary energy can be supplied as a combination of heat and electricity or solely by electricity.

Direct methanol synthesis

Methanol can be produced using CO_2 as a carbon source and H_2 through direct methanol synthesis (Eq. 14), avoiding the need for an elaborate reverse water–gas shift reaction (RWGS) to provide CO.

$$CO_2 + 3\ H_2 \rightleftharpoons CH_3OH + H_2O \tag{14}$$

The direct conversion of CO_2 and H_2 takes place under similar reaction conditions as in the conventional methanol synthesis. But, the per-pass conversion in direct methanol synthesis is thermodynamically limited to around < 45%; as a result, the unconverted reactants need to be recycled and fed back into the reaction zone to achieve higher overall

conversion rates, which adds complexity and cost to the process (Dieterich et al. 2020). According to Eq. 14, this methanol formation is accompanied by the formation of H_2O and is, therefore, associated with a higher separation effort compared to the conventional methanol synthesis.

Limitations of the chosen approach

In this study, a constant reference solar spectrum is assumed for all calculations, thereby neglecting the natural seasonal and diurnal variations that affect both photovoltaic (PV) electricity generation and photosynthetic biomass production. While this simplification allows for a direct comparison of energy conversion pathways under standardized conditions, it does not capture fluctuations in real-world energy yields that would result from changing sunlight intensity over the course of the day or year.

Furthermore, the analysis presented here is purely energy-based, focusing solely on the conversion of primary solar energy into usable methanol. Other critical factors that influence the feasibility and sustainability of each pathway (such as construction of the conversion plant, land-use requirements, capital expenditure, operational expenditure, water consumption, and broader environmental impacts) are not considered. Consequently, while the results provide insight into energy conversion efficiency, they do not offer a complete assessment of overall resource use or environmental performance.

Regarding the direct air capture (DAC) process, the model assumes a purely electrical energy supply for CO_2 separation. However, many existing DAC technologies rely on low- to medium-temperature heat, which can significantly reduce the electrical load. In this context, exploring the potential integration of waste heat from methanol synthesis or other industrial processes into the DAC system could enhance overall energy efficiency and reduce operational costs. Such integration represents an important avenue for future research and techno-economic optimization.

Energy efficiency assessment

The energy efficiency/the conversion losses are assessed for each of the steps described above. An approximation is first made based on the physically/chemically unavoidable energy losses (i.e., assessment of the theoretical efficiency). Then, based on the literature, the maximum at present technically achievable energy efficiency (i.e., present-day efficiency) is also provided.

All calculations were conducted using Python—the underlying data and code for the calculations are freely available (see (Tuschewitzki et al. 2025)).

For the efficiency calculation of the process steps "solar cell" and "photosynthesis," a defined solar spectrum is required. Here, the reference spectral irradiance based on ASTM G-173–03 (National Renewable Energy Laboratory 2024) is used (i.e., air mass (AM) of 1.5 (solar zenith angle of 48.2°), hemispherical radiation, an equator-facing plane tilted at 37° toward the Sun, albedo corresponding to a light sandy soil, clear sky conditions). The wavelength range covered is from 280 to 4 000 nm. This spectrum is normalized to an integrated power of 1 000 W m^{-2}. The solar irradiance (W m^{-2} nm^{-1}) and the photon flux (photons s^{-1} m^{-2} nm^{-1}) of this reference spectrum are shown in Fig. 1 as a function of wavelength.

Biomass-based pathway

Photosynthesis

Energy losses during photosynthetic carbon assimilation occur in various parts of the overall process so that the photosynthetic efficiency is ultimately in the single-digit percentage range related to the total incident radiation energy. When estimating the photosynthetic efficiency, the three different photosynthetic pathways of terrestrial plants must be taken into account (i.e., C_3, C_4 and crassulacean acid metabolism (CAM) photosynthesis). The designation of C_3 and C_4 photosynthesis is based on the observation that in the former, the first intermediate product of carbon fixation is a 3-carbon molecule, and in the latter, a 4-carbon molecule (Ehleringer and Cerling 2002). Below, only C_3 plants are considered, as these are by far the most common plants in moderate climatic zones. They are particularly well adapted to moderate temperatures, with a typical optimum range of approximately 15–25 °C. Accordingly, any statements regarding their efficiency are context-dependent and valid under the specific climatic assumptions chosen for the analysis.

Theoretical efficiency. The maximum photosynthetic efficiencies for C_3 plants were estimated in Zhu et al. (2008). Thereby, a number of simplifications were made (e.g., the actual photon flux was not taken into account when calculating the light absorption at photosynthetic systems I and II, and reflection losses were specified at a flat rate of 10% of the incident radiation). A recalculation avoiding such simplifications is therefore carried out. Additionally, the current carbon dioxide concentration (approx. 420 ppm (2023) (Lan et al. 2024)) is taken into account.

Photosynthetically active radiation. The solar spectrum used here comprises wavelengths from 280 to 4 000 nm (International Organization for Standardization 2022). But only a proportion of the total radiation reaching the ground can be used by the photosynthesis process. Mostly, the range between a wavelength of 400 and 700 nm is specified as the

photosynthetically active region (PAR) (Chen and Blankenship 2011).

The ratio of the total quantum energy within the PAR range to the total quantum energy reaching Earth's surface results in 43.0%, i.e., only this percentage of the sunlight's energy reaching the soil falls within the photosynthetically active range. However, not all of this energy can be used for photosynthesis due to the additional loss mechanisms described below, which continuously reduce the overall efficiency (see Table 1 in the supplementary material).

Degree of absorption. Reflection and transmission losses occur depending on a broad variety of biochemical and structural factors. Since even different plants of the same species often have very different canopy structures which change throughout the growing season (Gitelson et al. 2021), only estimates can be made of these losses. McCree (McCree 1972) investigated the degree of absorption of the leaves of 22 different plant species at different wavelengths within the PAR range. By multiplying the mean of the reported degrees of absorption by the corresponding wavelength-specific quantum energy, the degree of absorption of the incoming light energy can be calculated. The ratio between the average absorbed energy and the average quantum energy in the PAR range is 0.886; i.e., 11.4% of the incident radiation in the PAR range is reflected or transmitted. This reduces the proportion of incident solar radiation that can be used to build up biomass to 38.1%.

Photochemical efficiency. The two photosystems and the pigment pairs they contain within their reaction centers largely determine the photochemical efficiency. The light energy collected by pigments results in a promotion from the ground state to a higher excited state. (For more details, see supplementary material.) The respective energy can then be passed to the reaction center via an electron transport chain. However, the excited state can also return to the ground state by emitting heat. This is called non-photochemical quenching and occurs, among others, when the rate of energy delivered to the reaction center of photosystem II is greater than the rate of electron transport from photosystem II to photosystem I (Krüger and Grondelle 2017). The excited state could also return to the ground state by fluorescing. The photochemical efficiency can be determined approximately via the maximum light absorption of the pigment pairs P680 and P700 in the two reaction centers. The average amount of energy per mole of photons in the PAR range minus the above-mentioned absorption losses results in 218 kJ mol^{-1}.

To calculate the mean energy of an absorbed photon, the photon flux from 400 to 680 nm is integrated and multiplied by the corresponding energy uptake per photon at P680 (i.e., 176 kJ mol^{-1}). Photons with lower energy levels in the PAR range are assumed to be absorbed at P700, respectively, and another integration from 680 to 700 nm with multiplication of the photon energy at P700 (i.e., 171 kJ mol^{-1}) takes place. The resulting average energy per photon absorbed is 175.5 kJ mol^{-1}. The excess energy (42.5 kJ mol^{-1}) is assumed to be converted into heat or released by fluorescence. This means that 19.4% of the absorbed radiation cannot be used for photosynthesis. This reduces the proportion of incident solar radiation used to build up biomass to 30.7 %.

Carbohydrate synthesis. The efficiency of carbohydrate synthesis can be calculated from the ratio between the reaction enthalpy of photosynthesis (Eq. 5; $\Delta H_R = 2\,802$ kJ mol^{-1}) and the quantum energy absorbed to produce the required chemical energy for the course of the reaction. Since 48 photons are required to synthesize 1 molecule of glucose and the average absorbed photon energy within the reaction centers is 175.5 kJ mol^{-1}, this quantum energy accounts for 8424 kJ mol^{-1}. Therefore, during carbohydrate synthesis of C_3 plants, only 33.3% of the energy absorbed in the reaction centers can contribute directly to form glucose. This further reduces the proportion of solar radiation to be used to build up biomass to 10.2%.

Photorespiration. In the Calvin cycle, the enzyme RuBisCO (ribulose-1,5-bisphosphate carboxylase/oxygenase) is responsible for transferring the absorbed CO_2 to a sugar molecule (i.e., ribulose-1,5-bisphosphate). However, RuBisCO can also react with oxygen (O_2) instead of CO_2. While 2 molecules of 3-phosphoglycerate (PGA) are formed in the reaction with CO_2 (which are integrated into the Calvin cycle to ultimately form sugar), 1 molecule of PGA and 1 molecule of 2-phosphoglycolate are formed in the reaction with O_2. Within the photorespiration process, the latter is converted back to PGA; this requires energy and results in the release of CO_2 (i.e., 0.5 mol CO_2 per RuBisCO oxygenation). Therefore, photorespiration reduces the photosynthetic efficiency (Peterhansel et al. 2010). Each RuBisCO-catalyzed oxygenation consumes 3.5 ATP, while the RuBisCO-catalyzed carboxylation consumes 3 ATP (Walker et al. 2016). Based on the ratio of oxygenation to carboxylation (ϕ), the energy effort of photorespiration can be calculated. This ratio is significantly influenced both by temperature and the CO_2 concentration in the atmosphere (Eq. 15) (Zhu et al. 2008). In_O and In_C are the intercellular oxygen and carbon dioxide concentrations, respectively. In_O was assumed to be 210 mbar (corresponding to the oxygen concentration in the air), while In_C is assumed to be 0.252 mbar (corresponding to 60% of the current atmospheric carbon dioxide content of around 420 ppm (Lan et al. 2024; Sharkey 1988)).

$$\phi = \frac{In_O}{In_C \tau} \tag{15}$$

τ is the specificity factor of RuBisCO for carbon dioxide (i.e., the ratio of the probabilities of carboxylation to oxygenation) and can be calculated according to Eq. 16. $V_{C,max}$ and $V_{O,max}$ are the maximum rates of carboxylation

and oxygenation and K_C and K_O are the Michaelis–Menten constants for carbon dioxide and oxygen, respectively. These temperature-dependent values are calculated based on empirically determined formulas (Bernacchi et al. 2001) for a temperature of 15 °C (being approximately the mean global average temperature).

$$\tau = \frac{V_{C,max} K_O}{K_C V_{O,max}} \tag{16}$$

Based on the principles of RuBisCO oxygenation and carboxylation, Eq. 17 shows the decrease in carbon fixation efficiency (d_{pr}) by photorespiration. With the selected framework conditions (i.e., temperature of 15°C and carbon dioxide content of 420 ppm), this leads to a d_{pr} value of 27.4%; i.e., the proportion of incident solar energy that can be used to build up biomass is reduced to 7.4%. Increasing the ambient temperature to 30 °C would significantly increase d_{pr} to 48.7%.

$$d_{pr} = 1 - \frac{3(1 - 0.5\phi)}{3 + 3.5\phi} \tag{17}$$

Respiration. During cellular respiration, the energy-rich end products of photosynthesis (i.e., sugars) are oxidized in a sequence of processes including glycolysis, tricarboxylic acid cycle, and mitochondrial electron transport chains. Ultimately, this results in the formation of ATP and carbon dioxide. ATP serves as a universal energy source for building new plant structures, but also for repairing damage to the plant and for the active uptake of ions by the roots (Yamori et al. 2020). Carbon dioxide escapes back into the atmosphere; i.e., this carbon must be regarded as a further loss. The ratio of carbon dioxide released in cellular respiration to carbon dioxide converted in photosynthesis must be lower than 1 (otherwise, the plant would not be able to nourish itself) and varies greatly from 0.3 to 0.88 (Amthor 2000). Based on (Zhu et al. 2008), the minimum ratio of 0.3 is used for the calculation of the efficiency reduction. The proportion of incident solar energy that can be used to build up biomass thus falls to 5.2%.

Comparison with present-day efficiency. In addition to the factors determining the theoretical efficiency, the present-day efficiency depends also on a number of other factors (e.g., type and age of the plant, water supply, leaf structure and orientation, nutrient availability). Depending on a specific location, these additional factors vary greatly. Therefore, they cannot be included in such a theoretical investigation. However, the present photosynthetic efficiency can be determined by measuring the CO_2 exchange at different times for individual plants or plant communities (Field et al. 1989).

Based on such measurements, a present-day efficiency of around 1 to 2% was determined for C_3 plants during their active phase of the vegetation period (Éva et al. 2019). In the subsequent course of this paper, a value of 1% is assumed for the present-day efficiency of photosynthesis.

Synthesis gas production via anaerobic digestion

The conversion of biomass into usable synthesis gases can be realized in various ways. In the following, the synthesis gas production via anaerobic digestion, is energetically examined.

Theoretical efficiency. The energy losses based on an anaerobic digestion for the production of biogas and its subsequent conversion into usable synthesis gas are addressed below.

Anaerobic digestion. The theoretical biogas yield and its composition can be estimated based on the substrate's elemental composition (Eq. 6) (Buswell and Mueller 1952). In the case of glucose, carbon dioxide and methane are formed in equal parts and the reaction enthalpy is $-131.3\ \mathrm{kJ\ mol^{-1}}$, meaning that around 4.7% of the glucose's inherent energy is released in the form of heat.

Furthermore, the microorganisms realizing the anaerobic digestion process must survive and reproduce themselves. These losses account for around 7% of the substrates inherent energy (Gallert et al. 2015), leading to a theoretical maximum efficiency of around 88.3% for the anaerobic digestion step in relation to the biomass used.

Reforming and conditioning. The reforming of biogas occurs at high temperatures using oxidizing agents. The conversion efficiency primarily depends on the quality of the biogas used, the reforming method, and the integration of the respective reforming process into an overarching industrial system. If the energy is supplied solely from the biomass itself, autothermal tri-reforming can be considered suitable. Under the condition of an autothermal reaction ($\Delta H_R = 0$) and a required syngas ratio of 2 (the synthesis gas must theoretically have a stoichiometric composition (stoichiometric number (SN) according to Eq. 18; [X] is the molar fraction of X)), Eq. 19 is derived considering the atomic balances. However, since the CO_2 to CH_4-ratio is significantly lower in the feed gas compared to biogas, the excess CO_2 must be separated from biogas beforehand.

$$SN = \frac{[H_2] - [CO_2]}{[CO] + [CO_2]} \tag{18}$$

$$CH_4 + 0.045CO_2 + 0.433O_2 + 0.089H_2O \rightarrow 1.045CO + 2.089H_2 \tag{19}$$

The theoretical minimum energy required for gas separation can be calculated using the Gibbs free energy of mixing (ΔG_{mix}). This calculation assumes that the mixtures behave as an ideal gas (Sect. "Synthesis gas production via electrolysis and direct air capture").

- According to Eq. 6, biogas is assumed to have a CH_4 to CO_2-ratio of 1. But, the ratio in the feed gas used for autothermal tri-reforming is 0.045 according to Eq. 19. To reach such a ratio, an energy expenditure of 4.94 kJ mol^{-1} CH_4 for CO_2 separation from biogas is needed.
- For O_2 provision, a concentration of 21 vol - % in the ambient air, a separation rate of 90%, and a purity of 99.99 vol - % are assumed. This results in an energy expenditure of 3.95 kJ mol^{-1} CH_4.

Based on these energy expenditures for the considered equimolar biogas mixture, the theoretical maximum efficiency of biogas reforming and conditioning is 99% (based on the higher heating value (HHV) of CH_4).

Comparison with present-day efficiency. In the practical implementation of the aforementioned sub-steps, a number of further energy losses occur.

Anaerobic digestion. Equation 6 is only valid for easily degradable model substrates. Therefore, the biogas yield from a typical substrate mixture is usually significantly lower, as biomass also contains components difficult or impossible to be anaerobically degraded (e.g., lignin). In addition to biogas, a residue is produced, consisting mainly of water and non-anaerobically degradable substances still containing biogenic materials and thus being typically an energy loss.

In addition to that, there are also process-related losses (e.g., heating and stirring the fermenter, substrate supply, and digestate discharge). Typically, the present-day efficiency of such systems is between 45 and 66% (Pöschl et al. 2010).

Reforming and conditioning. With regard to gas reforming and conditioning in real processes, O_2 must be provided, for example, by air liquefaction requiring a separation effort of 200 to 300 kJ kg^{-1} O_2 (Castle 2002; Yadav and Mondal 2022). The CO_2 partially removed before the reforming step can be separated by different physical or chemical absorption technologies. Depending on the respective process, the required energy varies between 1 100 and 3 800 kJ kg^{-1} CO_2, whereby different proportions of electrical or thermal energy are supplied (Liebich et al. 2020). Further energy losses during reforming depend, e.g., on the degree of heat integration. Separating CO_2 and providing O_2 reduce the efficiency of real processes to around 96%. Considering further heat losses, the overall reforming and conditioning efficiency sums up to 80 to 92% (Bube et al. 2024a).

Synthesis gas production via thermochemical gasification

In the following, the synthesis gas production based on a thermochemical gasification is energetically examined.

Theoretical efficiency. Below, the energy losses for a thermochemical gasification and a subsequent conditioning step to produce a usable synthesis gas are discussed.

Thermochemical gasification. To assess the process' theoretical efficiency, oxygen and water are available as gasification agents and biomass is only converted into the products CO, H, and CO_2. Since the energy comes only from biomass, autothermal reforming is assumed. Here, CO_2 is separated afterward as an oxygen sink to enable a synthesis gas ratio of 2 (Eq. 18). The overall reaction equation (Eq. 20) is obtained by observing the stoichiometry.

$$\begin{aligned} &C_6H_{12}O_6 + 1.067\ O_2 + 0.577\ H_2O \\ &\rightarrow 3.289\ CO + 6.577\ H_2 + 2.711\ CO_2 \end{aligned} \tag{20}$$

As the process is assumed to be autothermal (no additional energy is added to or removed from the process), the theoretical efficiency is 100% for this (idealized) gasification reaction.

Gas Conditioning. The conditioning of the product gas takes place via CO_2 separation (purity of captured CO_2 99.99 vol - %, capture rate according to Eq. 20). Again, the theoretical energy effort results from Gibbs energy of mixing (Sect. "Synthesis gas production via anaerobic digestion"). The same has to be applied prior to gasification for O_2 provision from ambient air. Taking the respective energy demand into account (i.e., 26.9 kJ mol^{-1} $C_6H_{12}O_6$ for CO_2 separation and 9.8 kJ mol^{-1} $C_6H_{12}O_6$ for O_2 provision) results in a gas conditioning efficiency of 98.7%.

Comparison with present-day efficiency. The present-day energy efficiency achievable in synthesis gas production using thermochemical gasification and subsequent gas conditioning is presented below.

Thermochemical gasification. Due to an incomplete biomass transformation into the gas phase, energy requirements for drying and heat losses to the environment as well as numerous other unavoidable losses, gasification efficiencies of existing plants range between 60 and 75% (Kan et al. 2015).

Gas conditioning. Depending on the technology used and the heat integration within the overall plant, an efficiency of approx. 85 to 95% results for conditioning of gas from thermochemical gasification.

Conventional methanol synthesis

Theoretical efficiency. Methanol synthesis is an exothermic reaction; i.e., the energy content of the products is lower than that of the reactants. The reaction enthalpy of the conventional methanol synthesis from the product gases CO and H_2 (Eq. 12) is −90.6 kJ mol^{-1}. Hence, in relation to the calorific

value of the educts (i.e., CO and H_2, HHV = 283.0 kJ mol^{-1} and 285.8 kJ mol^{-1}, respectively), the efficiency is 85.0%. The 15% losses are returned as heat that could theoretically be used in other processes.

Comparison with present-day efficiency. In existing production plants, additional heat losses occur mainly due to impurities in the syngas, which must be purged in order to avoid accumulation (purge gas). The energy efficiency of present-day methanol synthesis processes, including separation and internal heat utilization, is around 78% (Bube et al. 2024b). Additional heat utilization in other processes could increase the overall efficiency.

Pathway efficiency

Based on the efficiencies of the various conversion steps presented above, the overall efficiency of methanol production can be calculated for the pathways under consideration. The results are presented below.

The upper part of Fig. 3 presents the theoretical efficiency in methanol production for the considered biomass-based pathways. While approx. 3.8% of the initially provided energy (i.e., terrestrial solar radiation) can be found in the final product within the theoretical consideration realizing synthesis gas provision via anaerobic digestion, this value is slightly higher (i.e., 4.4%) when the synthesis gas is provided via thermochemical gasification.

In the upper part of Fig. 4, the present-day efficiencies in methanol production are presented for the considered biomass-based pathways. Again, the efficiency realizing synthesis gas provision via thermochemical gasification is slightly more efficient compared to the option including synthesis gas provision via anaerobic digestion (0.40 to 0.56% and 0.28 to 0.47%, respectively).

Power-based pathway

Solar cell

Theoretical efficiency. The theoretical maximum efficiency of a solar cell can be calculated based on the "detailed balance" model ((Shockley and Queisser 1961), extended in Tiedje et al. (1984)). Due to the complexity of the extended model, here the simpler model by Shockley and Queisser (Shockley and Queisser 1961) is explained with a short explanation of the differences to the extended model (Tiedje et al. 1984). This model provides a clear framework for understanding the fundamental limits of single-junction solar cell efficiency, based on physical principles.

The model describes the theoretical maximum for a planar single-junction solar cell without concentrators or reflectors by balancing light absorption and radiative recombination (Shockley and Queisser 1961). The key assumptions are outlined below.

- Each photon with energy greater than the band gap energy $E_g = h\,\nu_g$ is absorbed (with Planck's constant h and the frequency of the wave ν_g at band gap energy) resulting in the ultimate efficiency.
- Infinite mobility of electrons and holes (no limitation of kinetics) is presumed.
- The material is perfect (i.e., no recombination other than radiative recombination (spontaneous emission of photons)).

The short-circuit current density (J_{SC}) and the dark saturation current density (J_0) of the solar cell are determined with Eq. 21 and Eq. 22, respectively. The formulas differ only in the geometric factor for irradiance ($f_w = 2.18 \cdot 10^{-5}$ and $f_0 = 1$ (Landsberg et al. 2005) and their temperature-dependent spectral flux ($\varphi(E_g, T)$), with the temperature at the surface of the Sun (T_S) for J_{SC} and the temperature of the solar cell (T_C) for J_0. q is the elemental charge ($1.602 \cdot 10^{-19}$ C). The efficiency of a solar cell is highly dependent on the band gap of the material used, as it directly influences these current densities by determining which photon energies contribute to charge generation.

$$J_{SC} = q f_w \varphi(E_g, T_s) \tag{21}$$

$$J_0 = q f_0 \varphi(E_g, T_c) \tag{22}$$

The spectral flux (φ) represents the radiation received per unit area and wavelength and can either be calculated according to Eq. 23 for a specific temperature, or a measured spectral flux can be utilized (e.g., the ASTM G-173–03 spectrum).

$$\varphi(T) = \frac{2\pi}{h^3\,c^2} \int_{E_g}^{\infty} \frac{E^2}{\exp\left(\frac{E}{k_B\,T}\right) - 1} dE \tag{23}$$

The current density (J), dependent on the operation voltage of the cell (V) and the thermal voltage of the cell (V_C) (Eq. 24), can be calculated according to Eq. 25.

$$k_B\,T_C = q\,V_C \tag{24}$$

$$J = J_{SC} + J_0\left(1 - \exp\left(\frac{V}{V_C}\right)\right) = J_{SC} + J_0\left(1 - \exp\left(\frac{qV}{k_B\,T_C}\right)\right) \tag{25}$$

By evaluating this equation in the interval from zero to the open-circuit voltage (V_{OC}, Eq. 26) (maximum voltage

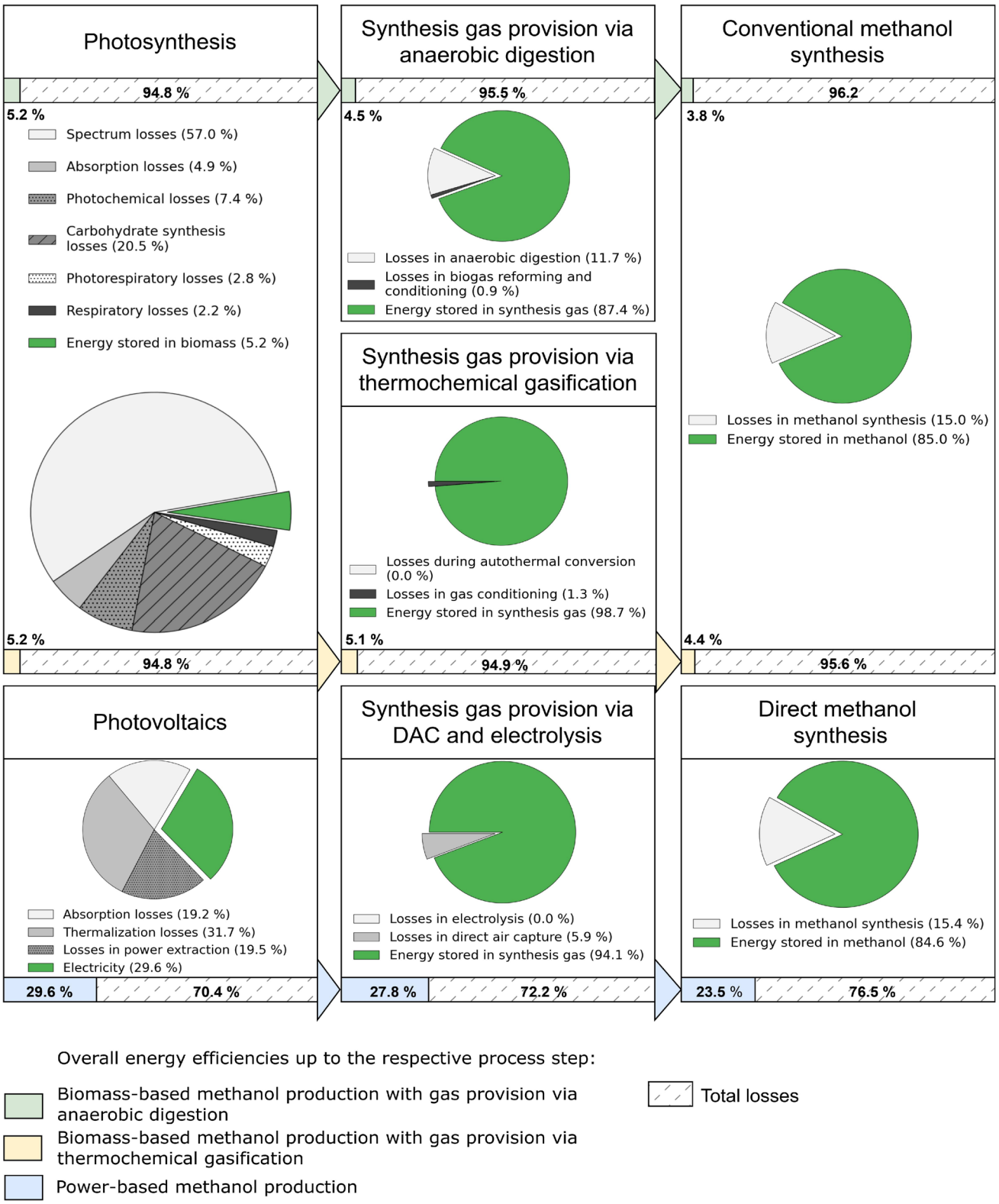

Fig. 3 Theoretical efficiencies and losses in the three considered methanol production pathways. Values for the overall energy efficiency represent energy flows as percentage of the terrestrial solar irradiation from the reference spectrum ASTM G-173–03, while values in the pie chart refer only to the respective process step

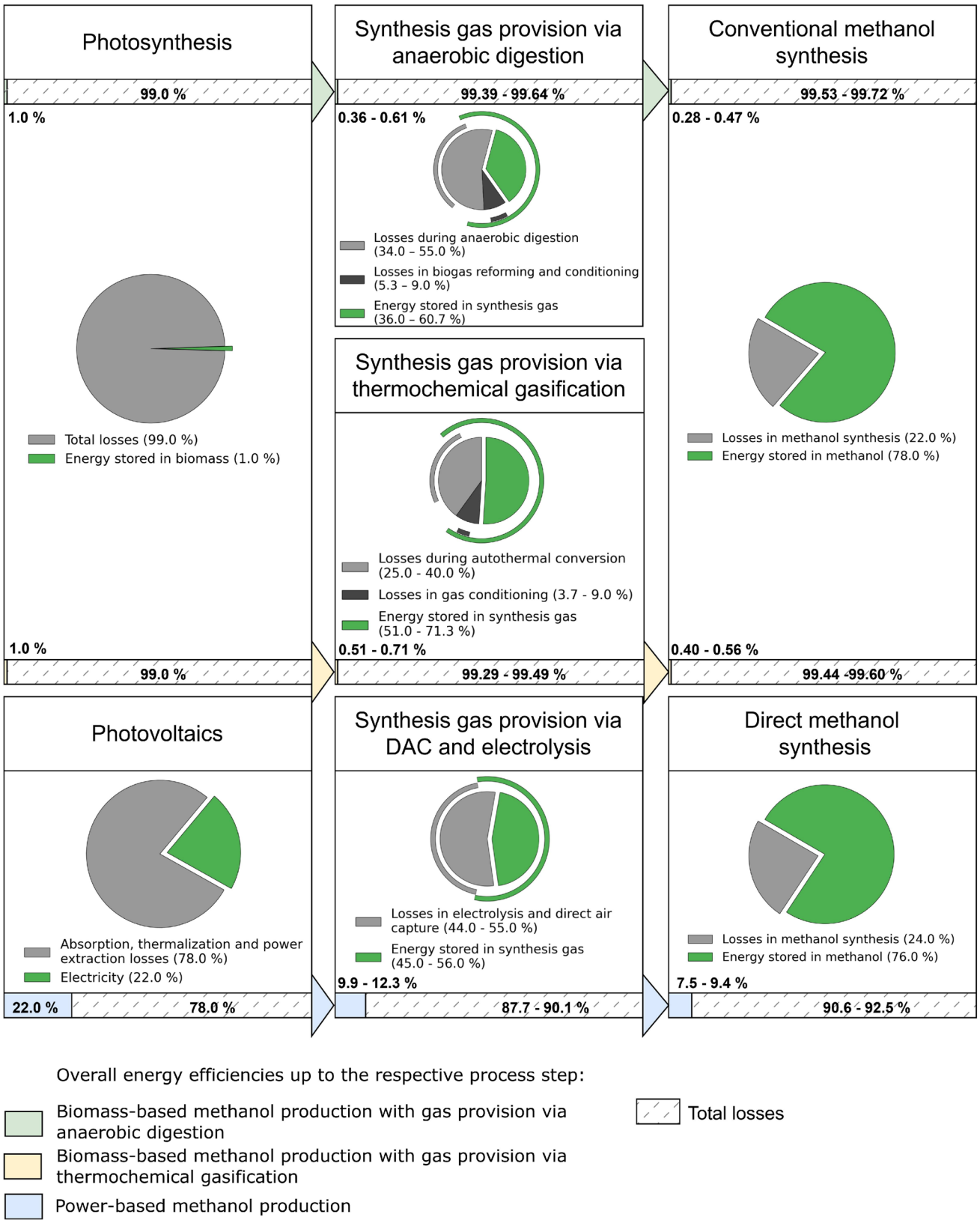

Fig. 4 Present efficiencies and losses in the three considered methanol production pathways. Values for the overall energy efficiency represent energy flows as percentage of the terrestrial solar irradiation from the reference spectrum ASTM G-173–03, while values in the pie chart refer only to the respective process step. If values are given as ranges, the lower value is displayed in the inner pie chart and the upper value in the outer ring

of a solar cell at 0 A), the maximum power point (*MPP*), with its corresponding voltage and current density (V_{MPP} and J_{MPP}), can be identified. (For additional information, check the supplementary material.) The efficiency of the detailed balance can then be determined by the quotient of the maximum power output of the solar cell and the incident power density (P_{inc}) (Eq. 27).

$$V_{OC} = V_C \ln\left(\frac{J_{SC}}{J_0} + 1\right) = \frac{k_B T_C}{q} \ln\left(\frac{J_{SC}}{J_0} + 1\right) \tag{26}$$

$$\eta = \frac{J_{MPP} V_{MPP}}{P_{inc}} \tag{27}$$

here, the maximum efficiency for a solar cell on Earth is calculated using the standard reference spectrum and standard conditions for solar cell calculations (cell temperature $T_C = 25°C$). Furthermore, the Shockley–Queisser limit considers only basic photon losses and radiative recombination, whereas the updated, extended detailed balance model (Tiedje et al. 1984) incorporates additional, non-avoidable Auger charge-carrier recombination and free carrier absorption. Thus, for a more realistic consideration, the model according to Tiedje et al. (1984) is utilized. The most important losses in solar cells are described below.

- Photon losses

  Below band gap: Photons with an energy smaller than the band gap are not absorbed and thus do not contribute to electricity generation.
  Above band gap: For photons with an energy greater than the band gap, the energy exceeding the band gap is converted to heat ("thermalization loss").

- Recombination losses

  Radiative: After photon absorption, electrons and holes can recombine before contributing to the current and are re-emitted as photons.
  Auger: An electron–hole pair recombines, and the excess energy is transferred to a third carrier (either an electron or a hole), resulting in its excitation.
  Shockley–Read–Hall: Electrons or holes are trapped at defect sites within the semiconductor material, leading to non-radiative recombination (Tiedje et al. 1984).

- Free carrier absorption: Absorption of photons by free carriers (electrons in the conduction band and holes in the valence band) leading to intra-band transitions and potential heating.
- Resistance losses

  Series: Ohmic resistance to the flow of current within the bulk material of the solar cell and the metal contacts.
  Shunt: Unintended parallel pathways for current flow within the solar cell allow bypassing the active junction of the solar cell. This is typically caused by defects or imperfections. A high shunt resistance is desirable.

- Optical losses

  Reflection: Photons are reflected and not absorbed (e.g., surface reflection, rear reflection).
  Transmission: Photons pass through the solar cell without being absorbed.

Many of these losses can be mitigated through advanced cell design and manufacturing techniques (e.g., anti-reflection coatings, Lambertian light-trapping (enhancing the optical path length of light through the material)). Some of the recombination radiation can also be reabsorbed (Tiedje et al. 1984). As a result, the practical limiting efficiency of single-junction silicon solar cells ($E_g = 1.12$ eV), based on the detailed balance model (Tiedje et al. 1984), is slightly below 30.0%. This limit has been refined over time with updated material properties (29.8% in 1984; 29.43% in 2013; and 29.56% in 2018 (Tiedje et al. 1984; Richter et al. 2013; Schäfer and Brendel 2018)). Additionally, this limit has nearly been reached with the present-day experimental record efficiency at $27.4 \pm 0.4\%$ (Green et al. 2025).

The lower part of Fig. 3 shows the energetic losses in photovoltaic electricity generation. For the detailed balance limit, the losses due to the not-absorbed photons amount to about 19.2% of the total energy. Losses due to thermalization amount to around 31.7% loss of the total energy (39.3% of the absorbed energy). Additionally, e.g., due to Auger recombination and free carrier absorption, further losses of about 19.5% occur (39.8% after non-absorption and thermalization) (Schäfer and Brendel 2018).

Comparison with present-day efficiency. When single cells are combined into a module, additional loss mechanisms must be considered, reducing the efficiency further. The most efficient single-junction silicon solar module reaches measured values of $25.4 \pm 0.3\%$ (Green et al. 2025), while present-day commercial mono-crystalline wafer-based silicon modules achieve efficiencies of roughly 22% (Fraunhofer Institute for Solar Energy Systems 2024). Given that silicon wafer-based solar cells account for about 97% of the total photovoltaic module production in 2023, with most of them being mono-crystalline cells (Fraunhofer Institute for Solar Energy Systems 2024), this type and its respective efficiency of 22% efficiency is used for calculations (Fig. 4).

Synthesis gas production via electrolysis and direct air capture

Hydrogen and carbon dioxide are required for direct methanol synthesis (Sect. "Direct methanol synthesis," Sect. "Direct methanol synthesis").

Theoretical efficiency. Here, the energy requirements of electrolysis and direct air capture are discussed. Then, these results are combined to calculate an overall efficiency.

Electrolysis. The minimum required energy for water electrolysis (Eq. 13) corresponds to the formation enthalpy (ΔH_R) of liquid water. This energy comprises Gibbs energy of reaction (ΔG_R) and the change in entropy (ΔS_R) multiplied by the corresponding temperature (T_R) (Eq. 28). The respective values depend on the temperature and, to a lesser extent, on the reaction pressure.

$$\Delta H_R = \Delta G_R + T_R \, \Delta S_R = \Delta G_R + \Delta Q_R \tag{28}$$

While the Gibbs energy must be supplied as electrical energy, the remaining energy can be provided as heat (ΔQ). The minimum cell voltage of an ideal, loss-free cell known as the reversible cell voltage (U_{rev}) can be calculated according to Eq. 29. In electrolysis cells, losses increase the cell voltage (U_{cell}; Eq. 31). They mainly arise due to required overvoltages to overcome voltage drops (Carmo et al. 2013; Buttler and Spliethoff 2018); this energy is mainly released as heat within the cell. The overvoltages can be categorized and described as follows.

- Overvoltage due to inherent ohmic resistance of electrodes, electrolyte, and connections (U_{ohm}), typically described with an Ohm's law equivalent resistor model (Carmo et al. 2013).
- Activation overvoltage (U_{act}) to start the electro-chemical reactions at the electrode surface, depending on the kinetics of the electron transfer reactions, can be described by the Butler–Volmer equation (Carmo et al. 2013).
- Concentration overvoltage (U_{con}), or mass transport overvoltage, occurs due to limitations in mass transport and changes in the concentration of reactants and products near the electrode surface compared to the bulk electrolyte. The overvoltage results from diffusion processes, often modeled using Fick's law, and it can be quantitatively related to concentration effects described by the Nernst equation, affecting the reaction rates, particularly at higher current densities (Carmo et al. 2013).

If the energy losses are equal to the heat requirement of the reaction, the cell can be operated thermoneutral. The thermoneutral cell voltage (U_{tn}) is calculated according to Eq. 30 and results in an efficiency of 100% (based on liquid water and the higher heating value of hydrogen ($HHV_{H_2} = 285.8\ \mathrm{kJ\,mol^{-1}} = 39.39\ \mathrm{kWh\,kg^{-1}}$)).

$$U_{rev} = \frac{\Delta G}{2\,F} \tag{29}$$

$$U_{tn} = \frac{\Delta H}{2\,F} \tag{30}$$

$$U_{cell} = U_{rev} + U_{ohm} + U_{act} + U_{con} \tag{31}$$

The maximum efficiency (η), taking into account the total energy to be supplied, is 100.0% based on the higher heating value.

Direct air capture. The minimum theoretical energy requirement (w_{min}) for the separation of a specific gas from a gas mixture can be calculated based on the reversible work required for their mixing (Gibbs free energy of mixing (Eq. 32)) (Sect. "Synthesis gas production via anaerobic digestion"). Assuming ideal gas behavior and thermal and mechanical equilibrium with the environment (i.e., all gas components have the same temperature and pressure), the enthalpy of mixing (ΔH_{mix}) is zero and the equation for Gibbs free energy change (ΔG_{mix}) simplifies to the product of temperature (T) and the entropy of mixing (ΔS_{mix}).

Based on this, the equation can be reformulated to Eq. 33, where n is the number of moles, R is the universal gas constant, T is the temperature, y_i is the mole fraction of component i (out of N components) in the mixture, and x_i is the mole fraction of component i in the separated state.

$$w_{min} = -\Delta G_{mix} = -\left(\Delta H_{mix} - T\,\Delta S_{mix}\right) \tag{32}$$

$$\Delta G_{mix,ideal} = n\,R\,T \sum_{i}^{N} y_i \ln\left(\frac{y_i}{x_i}\right) \tag{33}$$

The separation can further be described by a model with three streams: the initial gas mixture stream A and the output streams B and C. Stream B is CO_2 enriched, and stream C has a reduced CO_2 content. To determine the theoretical minimum work of separation relative to one mole of the removed component (here CO_2) on the basis of the mole fractions of CO_2 in streams A (y_A) and B (y_B) and the carbon capture rate CR (i.e., fraction of CO_2 in stream A that is separated and extracted through stream B) and the temperature T of the gas stream results in Eq. 35. This equation can be used to calculate the theoretical minimum work for complete or partial separation of gas from a gas mixture, whereby both the capture rate and the resulting purity of the separated gas can be adjusted. For readability, y_C is substituted (Eq. 34).

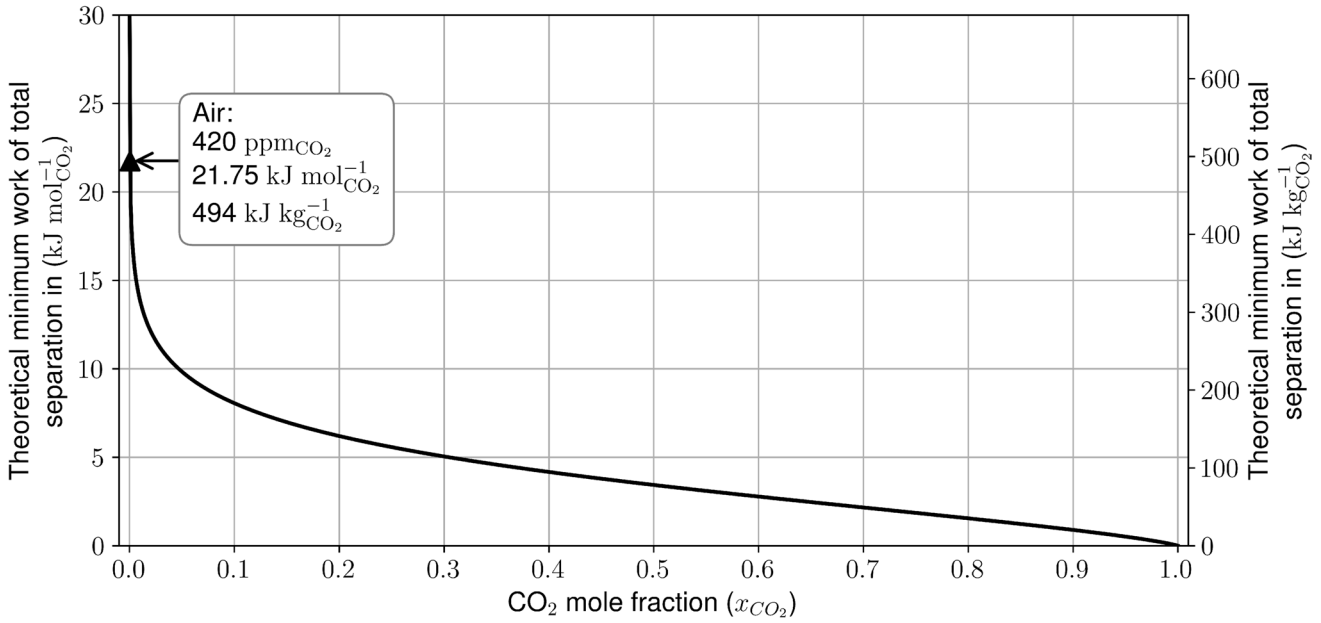

Fig. 5 Theoretical minimum work as a function of the mole fraction for the complete separation of a component from a gas mixture taking carbon dioxide (CO_2) as an example

$$y_C = \frac{y_A(1-CR)}{1-\frac{CR\,y_A}{y_B}} \tag{34}$$

$$\begin{aligned} &w_{min}(T, y_A, y_B, y_C, CR) \\ &\quad = \frac{\begin{aligned} &R\,T\,y_B\big(y_A\ln(y_A)+(1-y_A)\ln(1-y_A)\big) \\ &+\frac{CR\,y_A}{y_B}\big(y_B\ln(y_B)+(1-y_B)\ln(1-y_B)\big) \\ &-\left(1-\frac{CR\,y_A}{y_B}\right)\big(y_C\ln(y_C)+(1-y_C)\ln(1-y_C)\big) \end{aligned}}{CR\,y_A} \end{aligned} \tag{35}$$

In the context of DAC, where the goal is to separate CO_2 from air, the minimum required energy for CO_2 removal per mole (w_{min}) can be calculated by substituting $y_B = 1$, $y_C = 0$, $CR = 1$ in Eq. 35 to get a simplified equation (Eq. 36). An extensive deduction of the equations is provided in the supplementary material.

$$w_{min}(T, y_A) = -\frac{R\,T}{y_A}\big(y_A\ln(y_A)+(1-y_A)\ln(1-y_A)\big) \tag{36}$$

The theoretical minimum required energy for complete separation of CO_2 from ambient air (assumed to be an ideal gas at $T = 298.15$ K) is depicted in Fig. 5. The minimum work for total separation of CO_2 from ambient air at standard conditions with $y_A = 420$ ppm CO_2 is $w_{min} = 21.75$ kJ mol^{-1} of CO_2, resp. 137 kWh t^{-1} of CO_2.

In addition to the theoretical minimum energy of separation, DAC systems require energy for transporting the air into the separation unit (e.g., fans). Thus, an additional 31.68 kJ mol^{-1} of CO_2 (empirical data: 200 kWh t^{-1} of CO_2 (Fasihi et al. 2019), for further information check the supplementary material) is added, resulting in a theoretical minimum energy requirement of 53.43 kJ mol^{-1} of CO_2 (338 kWh t^{-1} of CO_2).

The CO_2 from the DAC is used together with the hydrogen from electrolysis to provide synthesis gas for methanol production. To generate one molecule of methanol (CH_3OH) via direct methanol synthesis (Sect. "Direct methanol synthesis"), one mole of CO_2 and three moles of H_2 are required (Eq. 14). To get the overall efficiency η_{syn}, the energy in the educts (CO_2, H_2) is divided by the energy required to generate these educts (Eq. 37).

$$\eta_{syngas} = \frac{3\,HHV_{H_2}}{w_{min,CO_2} + 3\,HHV_{H_2}\,\eta_{HHV}^{-1}} \tag{37}$$

This results in an efficiency of about 94.1% for the theoretical synthesis gas production via electrolysis and direct air capture (Fig. 3).

Comparison with present-day efficiency. The energy requirements of water electrolysis and direct air capture presently are clearly higher compared to the theoretical case.

Electrolysis. In present-day systems, additional energy is needed to overcome the overvoltages listed above. Consequently, the actual cell voltage is higher than the thermoneutral cell voltage (U_{tn}), leading to a reduced energy efficiency of about $\eta_{HHV} = 54$ to 71% for a complete electrolysis system

(including necessary auxiliary systems like pumps) (Buttler and Spliethoff 2018).

Direct air capture. For real gases, additional enthalpy is created in the process of mixing and due to irreversibilities of the separation process, leading to higher energy requirements for the removal of CO_2. Typically, DAC systems use a combination of heat and electricity; heat is mainly required for regenerating the sorbents. Here, all energy is assumed to be supplied as electric energy because electricity can be fully converted into heat.

For a low-temperature DAC (LT-DAC) system assumed here, the benchmark energy requirement is 1750 kWh_{th} and 250 kWh_{el} per t of separated CO_2 (Fasihi et al. 2019). This results in an estimated requirement of 316.80 kJ mol^{-1} of CO_2 (2000 kWh_{el} per t of CO_2), which is approximately six times the theoretical minimum energy demand (including energy requirements for the fan).

Based on these calculations, the synthesis gas provision with present-day efficiencies ranges from 45 to 56% considering the HHV value range of electrolysis (Fig. 4). Due to the low concentration of CO_2 in air, DAC is rather energy intensive. For the provision of the syngas yet, the energy efficiency of the hydrogen production plays a larger role since for the provision of methanol only one mole of CO_2 is required but 3 mol of H_2. Here, DAC makes up for about 9 to 15% points of the energy losses in syngas production.

Direct methanol synthesis

Theoretical efficiency. The reaction enthalpy of direct methanol synthesis from the product gases CO_2 and H_2 according to Eq. 14 is −49.2 kJ mol^{-1}. With respect to the calorific value of the educts (i.e., CO_2 and H_2, HHV = 0 kJ mol^{-1} and 285.8 kJ mol^{-1}, respectively), the theoretical efficiency is 84.7%, and the losses are released as heat that could theoretically be used in other processes.

The minimum energy requirement for the separation of water and methanol is 1320 kJ $kg^{-1}_{methanol}$. This corresponds to the excess enthalpy of mixing, determined by the non-random two-liquid (NRTL) activity coefficient model (Renon and Prausnitz 1968). Based on this, efficiency decreases only slightly to 84.6% (Fig. 3).

Comparison with present-day efficiency. Due to, among others, purge gas and additional heat losses, the efficiency of existing methanol synthesis plants is lower compared to theoretical values. Present-day plant efficiencies are assumed to be around 76% (Bube et al. 2024a). The lower efficiency compared to the conventional methanol synthesis is due to the higher water formation, and thus, the additional separation effort, as well as the lower per-pass conversion and the associated increased compression effort. It includes internal heat utilization for the water distillation. Additional waste heat utilization in other processes could increase the overall efficiency.

Pathway efficiency

The theoretical and present-day efficiencies for the overall power-based pathway are shown in the lower part of Figs. 3 and 4. Losses of the individual sub-steps within the major conversion steps (i.e., photovoltaic electricity provision, synthesis gas provision, and direct methanol synthesis) are depicted in gray, while the remainder per step is shown in green in the pie charts. The overall efficiency is shown as a bar and refers to the irradiated solar energy; for the complete power-based pathway, the overall theoretical efficiency is 23.5% and the overall present-day efficiency is 7.5 to 9.4%. Most of the energetic losses (> 70%) occur inside the solar cell. The subsequent losses are significantly smaller with 6.1% for theoretical efficiencies and 12.6 to 14.5% for present-day efficiencies.

The overall efficiency of the pathway with present-day process efficiencies is significantly smaller than for the process with theoretical efficiencies due to higher losses in the synthesis gas provision process (electrolysis and direct air capture).

Rationalization and discussion of the results

Below, the theoretically achievable energy efficiencies of the processes are first compared with each other, followed by a comparison with the energy efficiencies currently achievable in reality. Building on this, the impact of processing already available biomass is also considered. Finally, effects of a combination of the two cases under consideration are addressed.

Process efficiencies

Theoretical efficiency. The overall theoretical energy efficiency of the biomass-based pathway is 3.8% if the gas required for methanol synthesis is produced via anaerobic digestion and 4.4% if the gas comes from a thermochemical gasification process. In comparison, a much higher overall efficiency of 23.5% is achieved in the power-based process; i.e., the power-based pathway shows a clear advantage in terms of energy efficiency.

The comparatively low efficiency of the biomass-based pathway is mainly due to the relatively inefficient (natural) buildup of biomass via photosynthesis. This low efficiency stems from the fact that, over millions of years, nature prioritized resilience in photosynthetic systems rather than optimizing for energy efficiency, as humans do in technical systems. This evolutionary approach ensures species survival

even under suboptimal conditions. Because this fact is well known, efforts are on the way to increase photosynthesis efficiency (e.g., by incorporating novel chlorophylls into plants to extend the photosynthetically useable spectrum) (Evans 2013). An increase in photosynthetic efficiency of up to 30% is reported for individual measures (e.g., (Zhu et al. 2010)). However, even if such efforts were successfully implemented, it would not be possible to achieve such high theoretical efficiencies as in the power-based pathway (e.g., in a theoretical assessment, the photosynthetic efficiency would increase only to approximately 6.8%).

Nonetheless, it is important to recognize that, despite the above-mentioned drawbacks, biomass provides additional benefits beyond mere energy content. Acting as a naturally integrated carbon capture and storage system, it offers value that conventional energy-based metrics fail to reflect. In this context, another study has emphasized that evaluating organic matter solely on the basis of gross and net calorific values would be insufficient, as these metrics do not capture the work that nature performs to extract CO_2 from the atmosphere. This perspective highlights the importance of accounting for both the CO_2 separation and chemical reduction inherent in biomass formation, which contribute to its intrinsic value in ways that purely calorific assessments overlook. By acknowledging the energy-intensive processes that technical systems would need to replicate, the study underscores that biomass possesses a higher intrinsic worth than is typically recognized (Tuschewitzki et al. 2026).

Additionally, for the theoretical efficiency of the power-based pathway single-junction silicon cells with a maximum efficiency of 29.56% (Schäfer and Brendel 2018) are considered. Compared to that, multi-junction cells currently can already realize 47.6 ± 2.6% (Green et al. 2023) under laboratory conditions. Thus, by using multi-junction solar cells, the efficiency of the power-based pathway could clearly be further enhanced.

Comparison with present-day efficiency. Assuming the present-day efficiencies of the individual process steps reduces the overall efficiency of methanol production via the biomass-based pathway to 0.28 to 0.47% (via anaerobic digestion), or to 0.40 to 0.56% (via thermochemical gasification). This is significantly lower compared to the power-based pathway, where under current conditions an overall efficiency between 7.5 and 9.4% can be achieved. However, the strong influence of photosynthesis is also evident here. If photosynthesis is not included (e.g., because the biomass used as a feedstock is available as waste (e.g., organic household waste)), the energy efficiency for methanol production increases 100-fold to values of 28.1 to 47.4% (anaerobic digestion pathway) and 39.8 to 55.6% (thermochemical gasification pathway).

In the power-based pathway, the efficiency of the overall process route could be further improved through the utilization of high-temperature waste heat from the exothermal methanol synthesis for direct air capture. As outlined in Sect. "Limitations of the chosen approach," the embodied energy and construction of the plants are not included in this assessment; however, accounting for these contributions would not be expected to overturn the relative comparison between biomass- and power-based pathways.

Energetic evaluation of biomass

Conversion path-related value of biomass. In some cases, organic waste is easily accessible (e.g., as by-products from food processing), offering a natural synthesis precursor with already formed storable compounds. As a result, photosynthetic efficiency no longer needs to be considered in the process chain of the previously described bio-based pathways. Consequently, the following approach is proposed to assign a specific energetic value (V_{Bio}) to this synthesis preperformance. This value represents the exploitable added benefit of using such biomass for methanol production through the outlined pathways in comparison with the purely power-based pathway.

V_{Bio} is calculated through Eq. 38, using the overall efficiency of the power-based methanol production pathway (η_{PB}), the efficiency of synthesis gas provision in the biomass-based methanol production ($\eta_{SGP,Bio}$), and the efficiency of conventional methanol synthesis (η_{ConSyn}), shown in Figs. 3 and 4.

$$V_{Bio} = \frac{1}{\eta_{PB}} - \frac{1}{\left(\eta_{SGP,Bio}\eta_{ConSyn}\right)} \tag{38}$$

From a theoretical perspective, the purely power-based pathway requires an energy input of 4.2 kJ $kJ^{-1}_{CH_3OH}$. In comparison, utilizing available organic waste materials for syngas production via anaerobic digestion followed by methanol synthesis requires 1.3 kJ $kJ^{-1}_{CH_3OH}$; thus, approx. 2.9 kJ $kJ^{-1}_{CH_3OH}$ can be saved (these savings equal V_{Bio}). If anaerobic digestion is replaced by thermochemical gasification (e.g., for the feedstock straw), V_{Bio} increases to 3.1 kJ $kJ^{-1}_{CH_3OH}$. In this context, it should be noted that these calculations always assume glucose ($C_6H_{12}O_6$) as the initial biomass to ensure comparability. In reality, the composition of the biomass may deviate from this (e.g., $(C_6H_{10}O_5)$n for cellulose, $(C_5H_8O_4)$m for hemicellulose). This means that the numerical values for such biomasses would differ from the values given, although the order of magnitude remains comparable.

Considering present-day efficiencies, V_{Bio} is even higher. In this case, the power-based pathway requires 10.7 to 13.3 kJ to produce one kJ of CH_3OH. For syngas production via anaerobic digestion followed by methanol synthesis, the

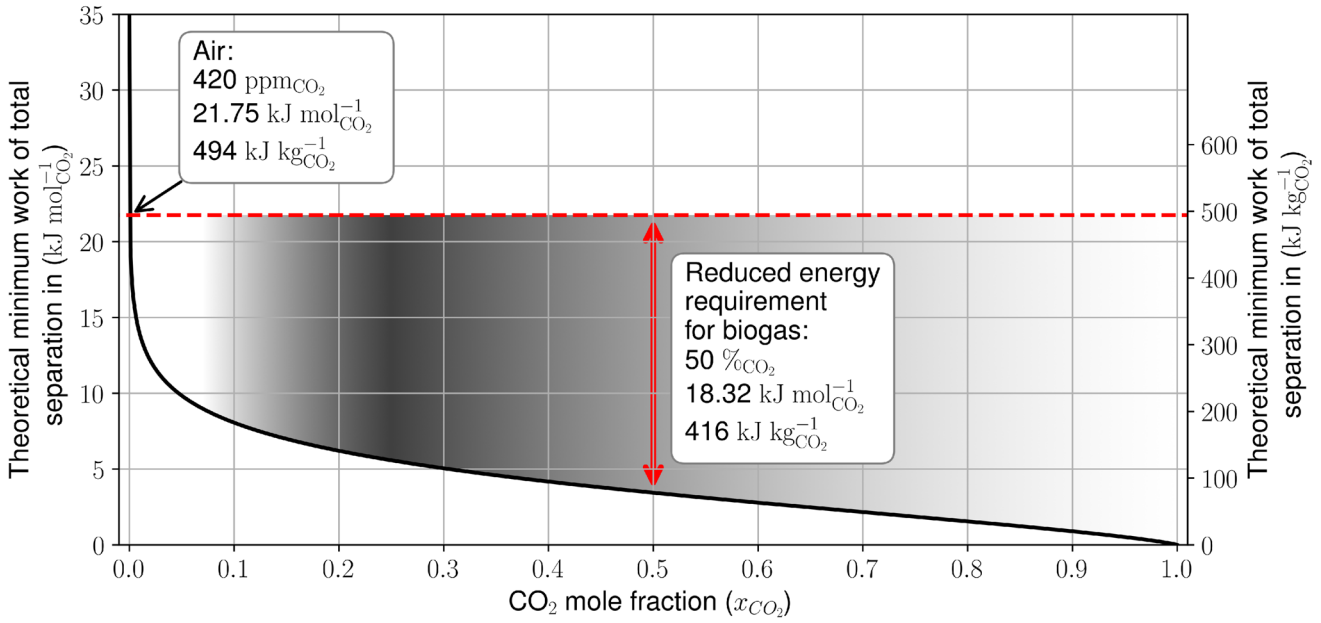

Fig. 6 Representation of potential energy savings in CO_2 capture from biogenic processes. The gray area represents the range in which the CO_2 fraction of biogenic gases lies (the darker the gray, the more common the CO_2-mole fraction in biogenic gases)

energy savings (i.e., V_{Bio}) are between 7.1 and 11.2 kJ $kJ^{-1}_{CH_3OH}$. In the case of syngas production via thermochemical gasification, V_{Bio} ranges from 8.2 to 11.5 kJ $kJ^{-1}_{CH_3OH}$. These higher values, compared to the theoretical estimates, primarily result from the fact that the syngas production in the power-based methanol production pathway is still far below its theoretical maximum.

The findings highlight that utilizing available organic waste streams/biomass waste can significantly reduce energy consumption in methanol production (i.e., the energy input can be reduced by up to approx. 7.4 times) compared to the reference pathway and favor the view of biomass as a valuable resource.

General added value of biomass. In addition to the previously considered energy efficiency benefits within the overall conversion pathway, biomass offers a remarkable advantage in terms of storability, which enables a more flexible use when converting it into methanol. The storage of organic waste materials does not require significant energy input; depending on the type of biomass, it can be kept in its natural state for extended periods without significant degradation. On the other hand, for the power-based pathway, energy storage can be realized via batteries or via hydrogen storage, which is typically more challenging compared to biomass storage. This added value for pathways using biomass cannot be quantified based on the assessment approach presented here.

Based on the results outlined above, a re-evaluation or reassessment of organic matter is warranted. Traditionally, organic material has been assessed based on its heating value. In a world where carbon, regardless of its origin, is essentially unlimited and where the resulting CO_2 emissions are of little concern, the heating value serves as a reasonable measure of its "value."

However, in a scenario where carbon is limited and its use is restricted to sources from the short-term carbon cycle, the work required to separate CO_2 from ambient air and chemically reduce it into easily storable long-chain carbohydrates gains additional significance. This separation process and preliminary synthesis work are not included in an evaluation solely based on the heating value.

Therefore, it is proposed to supplement the heating value by at least accounting for the energy required to separate CO_2 from the atmosphere (constituting to about 4.5% of the higher heating value of biomass (Tuschewitzki et al. 2026)). As a first approximation, this could be considered equivalent to the difference between the theoretical energy demand for CO_2 removal from air and the energy demand needed to separate CO_2 from biogenic sources with higher CO_2 concentrations (such as biogas or flue gas from solid biofuel combustion). This difference (i.e., separation value) is illustrated in Fig. 6 for a range found in gas streams containing biogenic CO_2 through the gray area. (The dark gray area represents the typical range in which the CO_2 fraction of biogenic gases lies.)

This means that if biogas with a CO_2 content of 50% is used instead of air in a DAC process, around 18.3 kJ $mol^{-1}_{CO_2}$ can be saved. If the produced compound (i.e., methanol in

the considered case) is finally also used for energy generation (i.e., combustion), the resulting exhaust gas could also provide additional benefits. For instance, with around 10 % of CO_2 in combustion air, this amounts to approximately 13.7 kJ $mol^{-1}_{CO_2}$. In the context of defossilization, biomass could thus prove to be advantageous if such CO_2 containing gases are further used.

Conclusion

In order to drive forward defossilization, there is an urgent need to find smart ways to continue producing carbon-containing products needed in the future based on a closed carbon cycle. The example of methanol as a carbon-based platform molecule is therefore used here to show how the energetic efforts of methanol production based on carbon dioxide from the atmosphere as a carbon source and sunlight via a biomass-based and a purely technology-based pathway look like. In addition to a description of the individual conversion processes, their theoretical maximum achievable energy efficiency is calculated. Then, a comparison with the energy efficiencies presently achievable in these processes is made. The key findings of this investigation are summarized below.

- The theoretical energy efficiency of biomass-based methanol production (i.e., 3.8 to 4.4 %) is significantly lower compared to that of a power-based methanol production (i.e., 23.5 %), provided that the buildup of biomass through photosynthesis is included in the calculation.
- A similar picture emerges for the present-day energy efficiencies (0.28 to 0.56 % overall energy efficiency for biomass-based methanol production; up to 9.4 % overall energy efficiency for power-based methanol production).
- If the photosynthesis efficiency is not taken into account, this picture changes (i.e., use of organic waste streams). In that case, biomass-based methanol production becomes much more efficient, ranging from a theoretical maximum energy efficiency of 74.3 to 83.9 % and a present-day energy efficiency of 27.4 to 47.4 %, depending on the type of gas provision during the conversion process (i.e., anaerobic digestion or thermochemical gasification).
- For the considered cases, a specific value can be assigned to biomass, derived from the differences in partial efficiencies during methanol production, reflecting potential energy savings in biomass-based methanol production compared to the power-based comparison case. This value lies between 2.9 and 3.1 kJ $kJ^{-1}_{CH_3OH}$ in the theoretical view and between 7.1 and 11.5 kJ $kJ^{-1}_{CH_3OH}$ under present-day conditions.
- In general, under the aforementioned conditions, the separation efforts of plants to remove CO_2 from the atmosphere and store them within organic material in a partly already chemically reduced way within CHO-molecule chains need to be taken into account, while describing the use of biomass as a carbon source to be used in a sustainable way within a closed loop within the short-term carbon cycle.

Another possibility for the energy efficient implementing of a methanol production could be a combination of the two processes presented. A number of positive effects could be achieved through such a combination.

- Electricity is required in both methanol production pathways, although the electricity requirement for the bio-based methanol production is significantly lower (i.e., only required for gas conditioning and reforming). If this electricity demand is not provided by photovoltaics, for example, the material utilization and thus the carbon use efficiency of the limited biomass could be increased.
- The conversion of organic matter into carbon-containing molecules via synthesis processes involves necessarily the removal of excess carbon and oxygen (in the form of CO_2) to achieve the required carbon-to-hydrogen ratio. By adding hydrogen from a power-based water splitting, the hydrogen deficit can be compensated without discharging carbon (as CO_2) from the overall process. This results in an efficiency increase compared to the separate production of biomass-based and electricity-based products.
- The combined utilization of biomass and power enables the shared use of downstream plant components (synthesis and processing), which could not only enhance efficiency but also could lead to cost reductions due to economies of scale. Additionally, it might open the door for the realization of high full load hours being impossible without the integration of additional storage facilities by utilizing solar energy.

Based on these results, it can be concluded that, from an energy efficiency perspective, only the use of organic waste materials for methanol production is prudent, while the cultivation of energy crops is clearly less promising. If biomass waste is available, this organic material should preferably be used compared to a solely power-based conversion pathway when considering only the energy aspect. Therefore, the use of organic residues, by-products, and wastes will gain significant importance in the years to come. Furthermore, power-based methanol production, with the required carbon

supplied through direct air capture (DAC), also presents an option that should not be overlooked from a purely energetic perspective.

Overall, by defining the theoretical maximum efficiencies of methanol production (3.8 to 4.4% (photosynthesis-based), 23.5% (power-based), and 74.3 to 83.9% (organic waste-based)), this work establishes a benchmark that future solar fuel technologies cannot surpass, providing a critical reference for guiding ongoing research.

Since, in addition to pure energy efficiency, other key figures such as production costs, land requirements, and GHG emissions play an important role in the realization of such production pathways, further investigations are necessary in order to be able to make holistic and fully justified recommendations.

Supplementary Information The online version contains supplementary material available at https://doi.org/10.1007/s10098-026-03468-x.

Author contribution Marvin Scherzinger contributed to conceptualization, data curation, formal analysis, methodology, visualization, and writing—original draft. Wolfram Tuschewitzki was involved in conceptualization, data curation, formal analysis, methodology, visualization, and writing—original draft. Stefan Bube contributed to formal analysis and writing—original draft. Martin Kaltschmitt was involved in conceptualization, supervision, and writing—review and editing.

Funding Open Access funding enabled and organized by Projekt DEAL. This research did not receive any specific grant from funding agencies in the public, commercial, or not-for-profit sectors.

Data availability The code for this study and all associated data is available on GitHub and Zenodo. Assessment and plotting: https://github.com/w-tusche/solar-energy-to-methanol, archived on Zenodo under https://zenodo.org/records/16884306.

Declarations

Conflict of interests The authors declare no competing interests.

Generative AI and AI-assisted technologies in the writing process During the preparation of this work, the authors used ChatGPT and Grammarly in order to improve readability and language. After using this tool/service, the authors reviewed and edited the content as needed and take full responsibility for the content of the publication.

References

Amthor J (2000) The McCree–De Wit–Penning de Vries–Thornley respiration paradigms: 30 years later. Ann Bot 86:1–20. https://doi.org/10.1006/anbo.2000.1175

Bernacchi CJ, Singsaas EL, Pimentel C et al (2001) Improved temperature response functions for models of rubisco–limited photosynthesis. Plant Cell Environ 24:253–259. https://doi.org/10.1111/j.1365-3040.2001.00668.x

Bube S, Sens L, Drawer C, Kaltschmitt M (2024a) Power and biogas to methanol – a techno-economic analysis of carbon-maximized green methanol production via two reforming approaches. Energy Convers Manag 304:118220. https://doi.org/10.1016/j.enconman.2024.118220

Bube S, Bullerdiek N, Voß S, Kaltschmitt M (2024b) Kerosene production from power-based syngas – a technical comparison of the Fischer-Tropsch and methanol pathway. Fuel 366:131269. https://doi.org/10.1016/j.fuel.2024.131269

Buswell AM, Mueller HF (1952) Mechanism of methane fermentation. Ind Eng Chem 44:550–552. https://doi.org/10.1021/ie50507a033

Buttler A, Spliethoff H (2018) Current status of water electrolysis for energy storage, grid balancing and sector coupling via power-to-gas and power-to-liquids: a review. Renew Sustain Energy Rev 82:2440–2454. https://doi.org/10.1016/j.rser.2017.09.003

Carmo M, Fritz DL, Mergel J, Stolten D (2013) A comprehensive review on PEM water electrolysis. Int J Hydrogen Energy 38:4901–4934. https://doi.org/10.1016/j.ijhydene.2013.01.151

Castle WF (2002) Air separation and liquefaction: recent developments and prospects for the beginning of the new millennium. Int J Refrig 25:158–172. https://doi.org/10.1016/S0140-7007(01)00003-2

Chen M, Blankenship RE (2011) Expanding the solar spectrum used by photosynthesis. Trends Plant Sci 16:427–431. https://doi.org/10.1016/j.tplants.2011.03.011

de Heer J (1957) The principle of Le Châtelier and Braun. J Chem Educ 34:375. https://doi.org/10.1021/ed034p375

Dieterich V, Buttler A, Hanel A et al (2020) Power-to-liquid via synthesis of methanol, DME or Fischer–Tropsch-fuels: a review. Energy Environ Sci 13:3207–3252. https://doi.org/10.1039/D0EE01187H

Ehleringer JR, Cerling TE (2002) C3 and C4 photosynthesis. Encyclopedia of Global Environmental Change 2:186–190

Éva C, Oszvald M, Tamás L (2019) Current and possible approaches for improving photosynthetic efficiency. Plant Sci 280:433–440. https://doi.org/10.1016/j.plantsci.2018.11.010

Evans JR (2013) Improving photosynthesis. Plant Physiol 162:1780–1793. https://doi.org/10.1104/pp.113.219006

Fasihi M, Efimova O, Breyer C (2019) Techno-economic assessment of CO_2 direct air capture plants. J Clean Prod 224:957–980. https://doi.org/10.1016/j.jclepro.2019.03.086

Field CB, Ball JT, Berry JA (1989) Photosynthesis: Principles and field techniques. In: Pearcey R (ed) Plant physiological ecology. Springer, Netherlands, Dordrecht, pp 209–253

Fraunhofer Institute for Solar Energy Systems (2024) Photovoltaics report. https://www.ise.fraunhofer.de/content/dam/ise/de/documents/publications/studies/Photovoltaics-Report.pdf [accessed on 18.04.2025].

Fulham GJ, Mendoza-Moreno PV, Marek EJ (2024) Managing intermittency of renewable power in sustainable production of methanol, coupled with direct air capture. Energy Environ Sci 17:4594–4621. https://doi.org/10.1039/D4EE00933A

Gallert C, Winter J, Svardal K et al (2015) Grundlagen anaerober Prozesse. In: Rosenwinkel K-H, Kroiss H, Dichtl N (eds) Anaerobtechnik. Springer Vieweg, Berlin; Heidelberg, pp 19–79

Gitelson A, Arkebauer T, Solovchenko A et al (2021) An insight into spectral composition of light available for photosynthesis via

remotely assessed absorption coefficient at leaf and canopy levels. Photosynth Res. https://doi.org/10.1007/s11120-021-00863-x
Green MA, Dunlop ED, Yoshita M et al (2023) Solar cell efficiency tables (version 62). Prog Photovoltaics Res Appl 31:651–663. https://doi.org/10.1002/pip.3726
Green MA, Dunlop ED, Yoshita M et al (2025) Solar cell efficiency tables (version 65). Prog Photovoltaics 33:3–15. https://doi.org/10.1002/pip.3867
International Organization for Standardization (2022) Solar energy. Reference solar spectral irradiance at the ground at different receiving conditions: Part 1: Direct normal and hemispherical solar irradiance for air mass 1,5. (ISO 9845–1:2022)
IPCC (2023) Climate change 2023: Synthesis report: A report of the intergovernmental panel on climate change. Contribution of working groups I, II and III to the sixth assessment report of the intergovernmental panel on climate change [core writing team, H. Lee and J. Romero (eds.)]. https://doi.org/10.59327/IPCC/AR6-9789291691647
Kan T, Strezov V (2015) Gasification of biomass. In: Strezov V, Evans TJ (eds) Biomass processing technologies. Taylor & Francis, Boca Raton, pp 81–121
Kar S, Kim D, Bin Mohamad Annuar A et al (2025) Direct air capture of CO_2 for solar fuel production in flow. Nat Energy 10:448–459. https://doi.org/10.1038/s41560-025-01714-y
Krüger TPJ, van Grondelle R (2017) The role of energy losses in photosynthetic light harvesting. J Phys B at Mol Opt Phys 50:132001. https://doi.org/10.1088/1361-6455/aa7583
Kweku D, Bismark O, Maxwell A et al (2018) Greenhouse effect: greenhouse gases and their impact on global warming. Journal of Scientific Research and Reports 17:1–9. https://doi.org/10.9734/JSRR/2017/39630
Lan X, Tans P, Thoning K, NOAA Global Monitoring Laboratory (2024) Trends in globally-averaged CO_2 determined from NOAA global monitoring laboratory measurements. https://doi.org/10.15138/9N0H-ZH07
Landsberg PT, Markvart T (2005) IIa-3 - ideal efficiencies. In: Markvart T, Castañer L (eds) Solar cells. Elsevier Science, Oxford, pp 57–68
Liebich A, Fröhlich T, Münter D, et al. (2020) System comparison of storable energy carriers from renewable energies. https://www.umweltbundesamt.de/publikationen/system-comparison-of-storable-energy-carriers-from [accessed on 18.04.2025]
McCree KJ (1972) The action spectrum, absorptance and quantum yield of photosynthesis in crop plants. Agricultural Meteorology 191–216.
Molino A, Chianese S, Musmarra D (2016) Biomass gasification technology: the state of the art overview. J Energy Chem 25:10–25. https://doi.org/10.1016/j.jechem.2015.11.005
National Renewable Energy Laboratory (2024) Reference air mass 1.5 spectra. https://www.nrel.gov/grid/solar-resource/spectra-am1.5.html [accessed on 18.04.2025]
Nelson J (2010) The physics of solar cells. Imperial College Press, London, Reprinted
Newton RG (1982). Scattering Theory of Waves and Particles. https://doi.org/10.1007/978-3-642-88128-2
Nugent JH (1996) Oxygenic photosynthesis. Electron transfer in photosystem I and photosystem II. Eur J Biochem 237:519–531. https://doi.org/10.1111/j.1432-1033.1996.00519.x
Ott J, Gronemann V, Pontzen F et al (2012) Methanol. Ullmann's Encyclopedia Ind Chem. https://doi.org/10.1002/14356007.a16_465.pub3
Peterhansel C, Horst I, Niessen M et al (2010) Photorespiration. Arabidopsis Book 8:e0130. https://doi.org/10.1199/tab.0130
Pöschl M, Ward S, Owende P (2010) Evaluation of energy efficiency of various biogas production and utilization pathways. Appl Energy 87:3305–3321. https://doi.org/10.1016/j.apenergy.2010.05.011
Prša A, Harmanec P, Torres G et al (2016) Nominal values for selected soalr and planetary quantities. Astron J 152:41. https://doi.org/10.3847/0004-6256/152/2/41
Puig-Arnavat M, Bruno JC, Coronas A (2010) Review and analysis of biomass gasification models. Renew Sustain Energy Rev 14:2841–2851. https://doi.org/10.1016/j.rser.2010.07.030
Renon H, Prausnitz JM (1968) Local compositions in thermodynamic excess functions for liquid mixtures. AIChE J 14:135–144. https://doi.org/10.1002/aic.690140124
Richter A, Hermle M, Glunz SW (2013) Reassessment of the limiting efficiency for crystalline silicon solar cells. IEEE J Photovoltaics 3:1184–1191. https://doi.org/10.1109/JPHOTOV.2013.2270351
Rodriguez-Pastor DA, Soltero VM, Chacartegui R (2025) Green methanol production from photovoltaics in Europe. Renew Energy 254:123751. https://doi.org/10.1016/j.renene.2025.123751
Schäfer S, Brendel R (2018) Accurate calculation of the absorptance enhances efficiency limit of crystalline silicon solar cells with lambertian light trapping. IEEE J Photovoltaics 8:1156–1158. https://doi.org/10.1109/JPHOTOV.2018.2824024
Sharkey TD (1988) Estimating the rate of photorespiration in leaves. Physiol Plant 73:147–152. https://doi.org/10.1111/j.1399-3054.1988.tb09205.x
Shockley W, Queisser HJ (1961) Detailed balance limit of efficiency of p-n junction solar cells. J Appl Phys 32:510–519. https://doi.org/10.1063/1.1736034
Tiedje T, Yablonovitch E, Cody GD, Brooks BG (1984) Limiting efficiency of silicon solar cells. IEEE Trans Electron Devices 31:711–716. https://doi.org/10.1109/T-ED.1984.21594
Tuschewitzki W, Scherzinger M, Bube S (2025) Solar-energy-to-methanol (0.1.0). Zenodo. https://doi.org/10.5281/zenodo.16884306
Tuschewitzki WG, Scherzinger M, Kaltschmitt M (2026) Reassessment of the energetic value of lignocellulosic biomass in closed carbon cycles. Biomass Bioenergy 206:108581. https://doi.org/10.1016/j.biombioe.2025.108581
Uddin MM, Wright MM (2023) Anaerobic digestion fundamentals, challenges, and technological advances. Phys Sci Rev 8:2819–2837. https://doi.org/10.1515/psr-2021-0068
Walker BJ, VanLoocke A, Bernacchi CJ, Ort DR (2016) The costs of photorespiration to food production now and in the future. Annu Rev Plant Biol 67:107–129. https://doi.org/10.1146/annurev-arplant-043015-111709
Würfel P (2010) Physics of solar cells: From basic principles to advanced concepts, 2., updated and expanded ed., 2. reprint. Wiley-VCH, Weinheim
Yadav S, Mondal SS (2022) A review on the progress and prospects of oxy-fuel carbon capture and sequestration (CCS) technology. Fuel 308:122057. https://doi.org/10.1016/j.fuel.2021.122057
Yamori W (2020) Photosynthesis and respiration. In: Kozai T, Niu G, Takagaki M (eds) Plant factory. Elsevier Academic Press, London; San Diego; Cambridge; Oxford, pp 197–206
Zhang M, Ge B, Gan Z et al (2025) Integrated power to methanol processes with steam-assisted direct air capture. Energy Convers Manag 326:119505. https://doi.org/10.1016/j.enconman.2025.119505
Zhao N, Yang J, Ai T, Wang J (2025) From methanol to power: energy, economic and life-cycle assessments of several pathways. J Clean Prod 486:144501. https://doi.org/10.1016/j.jclepro.2024.144501
Zhu X-G, Long SP, Ort DR (2008) What is the maximum efficiency with which photosynthesis can convert solar energy into biomass? Curr Opin Biotechnol 19:153–159. https://doi.org/10.1016/j.copbio.2008.02.004
Zhu X-G, Long SP, Ort DR (2010) Improving photosynthetic efficiency for greater yield. Annu Rev Plant Biol 61:235–261. https://doi.org/10.1146/annurev-arplant-042809-112206